

Graph-based Facial Affect Analysis: A Review of Methods, Applications and Challenges

Yang Liu^{1,2} · Xingming Zhang¹ · Jinzhao Zhou¹ · Xin Li¹ ·
Yante Li² · Guoying Zhao² · Yue Li¹

Received: date / Accepted: date

Abstract Facial affect analysis (FAA) using visual signals is a key step in human-computer interaction. Early methods mainly focus on extracting appearance and geometry features associated with human affects, while ignore the latent semantic information among individual facial changes, leading to limited performance and generalization. Recent trends attempt to establish a graph-based representation to model these semantic relationships and develop learning frameworks to leverage it for different FAA tasks. In this paper, we provide a comprehensive review of graph-based FAA, including the evolution of algorithms and their applications. First, we introduce the background knowledge of facial affect analysis, especially on the role of graph. We then discuss approaches that are widely used for graph-based affective representation in literature and show a trend towards graph construction. For the relational reasoning in graph-based FAA, we categorize the existing studies according to their usage of traditional methods or deep models, with a special emphasis on latest graph neural networks. Performance comparisons of the state-of-the-art on various FAA problems are also summarized. Finally, we discuss the challenges and potential directions. As far as we know, this is the first survey of graph-based

FAA methods, and our findings can serve as a reference point for future research in this field.

Keywords Facial Affect Analysis · Facial Expression Recognition · Micro-expression Recognition · Action Unit Detection · Affective Graph Representation · Graph Neural Network

1 Introduction

Facial affects are one of the most important visual signals for developing human-computer interaction systems, because it conveys critical information that reflects emotional states and reactions in human communications (Darwin and Prodger 1998; Gazzaniga et al. 2006; Picard et al. 2001). During the past decade, many facial affect analysis (FAA) methods have been explored based on interdisciplinary progresses of computer vision, cognitive neuroscience and psychology (Jack et al. 2012; Sariyanidi et al. 2014; Calvo et al. 2018). And some of them have been extended to various applications including diagnosis (Tavakolian and Hadid 2019), social media (Zhang et al. 2018b) and video generation (Zhao et al. 2020). Despite the successes, there are still some challenging gaps, such as coarse-grained to fine-grained affective representation, constrained to in-the-wild affect prediction, and discrete affect recognition to continuous affect intensity estimation.

Before going into the field of FAA, we need first to know what the facial affect is. As early as 1970s, Paul Ekman (Ekman and Friesen 1971) proposed the definition of six basic emotions, i.e., *happiness*, *sadness*, *fear*, *anger*, *disgust*, and *surprise*, based on an assumption of the universality of human affective display (Ekman 1994). This definition has been followed for many

✉ Yang Liu
E-mail: liuy17@163.com; yang.liu@oulu.fi

✉ Guoying Zhao
E-mail: guoying.zhao@oulu.fi

✉ Yue Li
E-mail: liyue@scut.edu.cn

¹ School of Computer Science and Engineering, South China University of Technology, Guangzhou, 510006, China

² Center for Machine Vision and Signal Analysis, University of Oulu, Oulu, FI-90014, Finland

years till now. Besides, another popular affect description model, called the Facial Action Coding System (FACS), was designed for a wider range of emotions, which consists of a set of atomic Action Units (AUs) (Friesen and Ekman 1978; Ekman 2002). Figure 1 shows an example of six basic emotions plus *neutral* as well as activated AUs in each facial affect. Both the two affective models are categorical one that depicts discrete human emotions. There are other findings suggesting a dimensional affective model (Plutchik 1980; Greenwald et al. 1989; Russell 1978), with valence and arousal (V-A), which is considered more appropriate to describe dynamic changes of human affects in real world.



Fig. 1 An example of basic facial affects and related AU marks. AU0 denotes no activated AU. Images are from BU-4DFE (Yin et al. 2008). From left to right: anger, disgust, fear and neutral (top); happiness, sadness and surprise (bottom).

In the community of computer vision and affective computing, several competitions (challenges) are held periodically to evaluate the latest progresses of FAA and propose frontier research trends. The Facial Expression Recognition and Analysis challenge (FERA) (2011, 2015, 2017) focuses on AU detection and emotion recognition (Valstar et al. 2011), and gradually introduces more complex factors such as intensity estimation and non-frontal head poses (Valstar et al. 2015). Moreover, the Emotion Recognition in the Wild challenge (EmotiW) (2013-2020) (Dhall et al. 2020), the Faces in-the-wild Challenge (Wild-Face) (2017) (Zafeiriou et al. 2017) and the EmotioNet Challenge (ENC) (2017, 2018, 2020) (Benitez-Quiroz et al. 2017) pay attention to discrete or continuous facial affects in real world scenarios. Besides, the Audio/Visual Emotion Challenge (AVEC) (2011-2019) (Ringeval et al. 2019) and the Multimodal Sentiment in Real-life Media (MuSe) Challenge (2020) (Stappen et al. 2020) aim at analyzing human sentiment in a multi-modality manner. These competitions also

provide universal annotated data and standard benchmarks that promote the development in FAA field.

Accordingly, FAA methods have experienced a series of historical evolution. Initial studies mostly rely on hand-crafted features or classic machine learning to obtain useful affective information (Sariyanidi et al. 2014). With the wave of the deep learning, the performance of various FAA tasks has been promoted into a higher level without tedious feature design and selection. Nevertheless, these methods often use raw images or simple facial partitions. They ignore key context and latent semantic information in facial affects (Bimler and Paramei 2006), which limits effectiveness and capability. Thus, a good facial affective representation is crucial for optimizing the feature learning process. Recently, graph-based FAA has received increasing attention, not only because it has more consistent representation with facial muscle anatomical definition (Mohseni et al. 2014), but also it is easier to encode prior knowledge for advanced affective features by using the graph structure.

In this paper, we review the state of research on FAA using graph-based methods. Although there are many reviews that have discussed the historical evolution (Sariyanidi et al. 2014; Corneanu et al. 2016; Martinez et al. 2017) and recent advances (Kollias et al. 2019; Li and Deng 2020; Goh et al. 2020) of FAA, including some on specific problems like occlusion expression (Zhang et al. 2018a), multi-modal affect (Rouast et al. 2019) and micro-expression (Ben et al. 2021), this is the first systematic and in-depth survey of the graph-based FAA field, as far as we know. We emphasize the research proposed after 2005, and focus on evaluating the state-of-the-art work. The goal is to present a novel perspective on FAA and its latest trend.

This paper is organized as follows: Section 2 introduces a generic pipeline of FAA and briefly discusses facial preprocessing methods. Section 3 presents a taxonomy of mainstream graph-based methods for facial representation. Section 4 reviews traditional and advanced approaches of graph relational reasoning and discusses their pros and cons in FAA tasks. The comments of commonly used public FAA databases are given in Section 5. Section 6 summarizes main FAA applications and current challenges based on a detailed comparison of related literature. Finally, Section 7 concludes with a general discussion and identifies potential directions.

2 Facial Affect Analysis

2.1 General Pipeline

A standard FAA method can be broken down into its fundamental components: facial preprocessing, affective

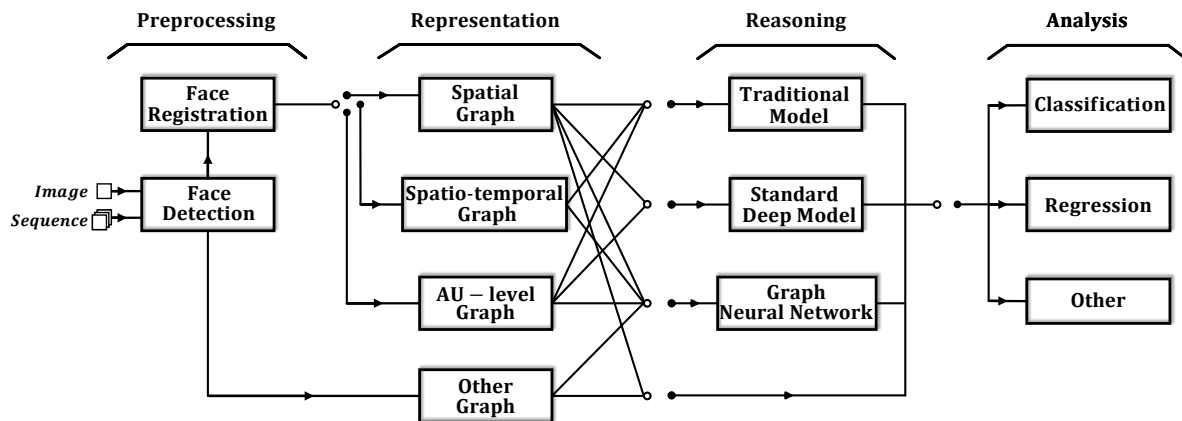


Fig. 2 The pipeline of graph-based facial affect analysis methods.

representation and task analysis. As a new branch of FAA, the graph-based method also follows this generic pipeline (see Fig. 2). Regarding the first two steps, many of their approaches can be used and shared when implementing various FAA tasks, while others are coupled with a certain logic according to previous outputs and next goals. Specifically, comparing to other existing FAA methods, the graph-based FAA pays more attention to how to represent facial affects with graphs and how to obtain affective features from such representation by graph reasoning. Naturally, depending on different affective graph representations, generic approaches need to be adjusted or new graph-based approaches are proposed to infer the latent relationship and generate the final affective feature. The introduction of graph neural networks (*GNNs*) is an example. Hence, advantages and limitations of different graph generation methods and their relational reasoning approaches are two main topics of this survey.

2.2 Role of Graph

As mentioned above, it is meaningful to use graphs to represent and analyze the structural information in facial affects. In mathematical terms, a graph can be denoted as $G = (V, E)$, where the node set V contains all the representation of the entities in the affective graph and the edge set E contains all the relations between two entities. For the sake of computation, the two sets commonly exist in the form of matrices. The edge set E is often represented as an adjacency matrix A where each element A_{ij} attributes for a degree of relation between the node N_i and N_j . The node set V is represented as the feature matrix H where each vector H_i in H is the feature representation of a node N_i .

Apparently, all the structure information of a graph is contained in E . Thus, when E is empty, G becomes

an unstructured collection of entities. Given this unstructured collection, performing relational reasoning requires the model to infer the structure of the entities at a higher order before predicting the property or category of an object. Meanwhile, we could also define some initial graph structure ahead of the relational model, which is a general practice in many affective graph representations. With richer information being manually or automatically provided through prior knowledge, the graph-based FAA methods are expected to exhibit better performance and generalization capability.

2.3 Preprocessing

Face detection is a necessary pre-step before conducting any kinds of FAA. It aims to first locate faces presented in raw images, and then obtain their bounding boxes. Early work usually utilizes Viola and Jones (Viola and Jones 2001), a cascade of weak classifiers, but its performance decreases when facing head-pose variations. Recently, deep learning methods are used for high speed and accuracy. For instance, the Multi-Task Cascaded Convolutional Network (*MTCNN*) exploits a deep cascaded architecture with a multi-task strategy that can quickly output aligned face and five facial landmarks (Zhang et al. 2016), and is widely used in FAA research. The *CenterFace* is another state-of-the-art face preprocessing algorithm, which predicts facial box and landmark location simultaneously (Xu et al. 2020a). It is more efficient than *MTCNN* when handling multi-subject face images, and thus suitable for images under complex conditions. The reader is referred to (Masi et al. 2018) for an extensive review on face detection methods.

Once the bounding box is located, it is enough for many FAA methods to perform feature learning. However, one additional procedure called face registration

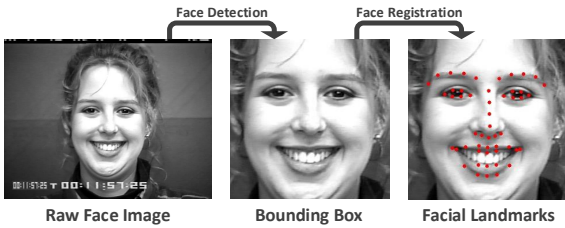


Fig. 3 An illustration of face detection and face registration. The *happy* image is from CK+ database (Lucey et al. 2010).

is meaningful to improve the FAA performance (Molahosseini et al. 2016; Khorrani et al. 2016). With this step, facial landmarks or face geometry are obtained to transform an input face into a prototypical face, which normalizes face variations and corrects the in-plane rotation. Although several methods (e.g., *MTCNN* and *CenterFace*) deal with face detection and face registration at the same stage, a transformation computed from more landmarks could be more comprehensive and less sensitive to individual landmark errors, which is crucial for a graph-based affective representation. The Active Appearance Model (*AAM*) is one of the classic methods for both whole face and parts (e.g., eyes, nose, mouth) registration (Cootes et al. 2001). However, the performance of *AAM* decreases heavily in real-world scenarios, including head-pose variations and partial occlusions. To this end, Mixtures of Trees (*MoT*) (Zhu and Ramanan 2012), a popular part-based face registration method, is employed to cope with in-the-wild conditions (Yu and Zhang 2015). Alternatively, some cascaded deep models with real-time performance are drawing attention in recent years (Ranjan et al. 2017; Feng et al. 2017). Unsupervised approaches such as Supervision by Registration and Triangulation (*SRT*) (Dong et al. 2020) are also explored for enhanced landmark detection in multi-view images and videos. Figure 3 presents an illustration of the preprocessing steps. A thorough review on this subject is out of the scope of this paper, the reader is referred to Bulat and Tzimiropoulos (2017) and Wang et al. (2018) for more details.

3 Graph-based Affective Representations

Affective representation is a fundamental procedure for most graph-based FAA methods. Depending on the domain that an affective graph models, we categorize the strategy as spatial graph, spatio-temporal graph, AU-level graph and others. Figure 4 illustrates a detailed summary of literature using different graph representations. Note that many graph-based representations contain pre-extracted geometric or/and appearance fea-

tures. Whether it is hand-crafted or learned, these feature descriptors are not essentially different from those used in non-graph-based affective representations. Interested readers can refer to Sariyanidi et al. (2014), Corneanu et al. (2016) and Li and Deng (2020) for a systematic understanding of this topic.

3.1 Spatial Graph Representations

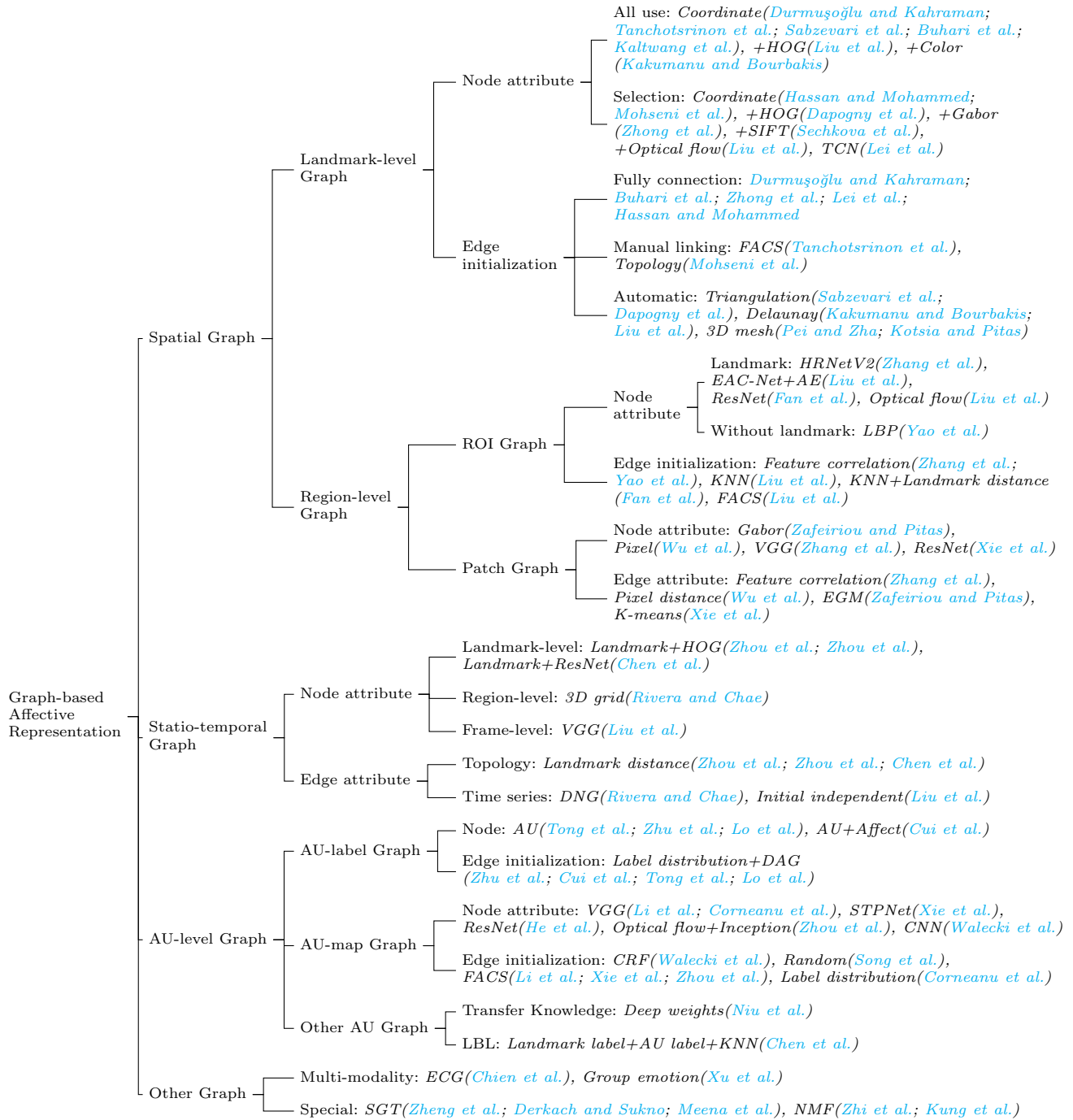
Spatial representations aim to encode facial geometry or appearance from an affective face. Generic spatial methods treat a facial affect as a whole representation or pay attention to variations among main face components or crucial facial parts (Zhao et al. 2016; Zhang et al. 2017; Oh et al. 2018). For graph-based spatial representations, not only facial changes are considered, but also their co-occurrence relationships and affective semantics are regarded as important cues for FAA (Yao et al. 2015; Zhong et al. 2019; Lei et al. 2020). The approaches used to generate spatial affective graphs can be divided into landmark-level graphs and region-level graphs. Figure 6 illustrates frameworks of different spatial graph representations.

3.1.1 Landmark-level graphs

Facial landmarks are one of the most important geometric information that reflects the shape of face components and the structure of facial anatomy. An illustration is shown in Fig. 5. Thus, it is a natural idea to use facial landmarks as base nodes for generating a graph representation. Note that facial shape is not the only information that landmark-level graphs encodes, facial appearances like color (Kakumanu and Bourbakis 2006) and texture (Sechkova et al. 2016) are also exploited to enrich landmark-level graphs.

Limited by the performance of landmark detection algorithms, only a few landmarks are applied in early graph representations. Tanchotsrinon et al. (2011) constructed a facial graph based on 14 landmarks located at regions of three eyebrow parts, two eye parts and mouth. Similarly, Durmuşoğlu and Kahraman (2016) utilized 18 landmarks to describe the geometric information attached to basic face components. Recently, graph representations using more facial landmarks are proposed to depict fine-grained facial shapes. Sabzevari et al. (2010) introduced constrained local model to search 60 related facial landmarks and then established a similarity normalized graph with a raw vector of landmark coordinates. The 68 landmarks detected by *dlib* library (Kazemi and Sullivan 2014) or the 66 landmarks provided by *AAM* are also widely used in the graph construction. For example, in Liu et al. (2019) and

Fig. 4 Taxonomy for Graph-based Facial Representation.



Buhari et al. (2020), the authors associated the 68 landmarks with the AUs in FACS and made graph-based representations. The difference is that the former additionally employed local appearance features extracted by Histograms of Oriented Gradients (*HOG*) (Dalal and Triggs 2005; Carcagnì et al. 2015) as attributes of nodes, while the latter proposed two strategies, *full-face graph* and *FACS-based graph*, for enhanced geometric repre-

sentations. Specially, Kaltwang et al. (2015) formulated a Latent Tree (*LT*) where 66 landmarks were set as part of leaf nodes accompanied by several other leaf nodes of AU targets and hidden variables. This graphical model represented the joint distribution of targets and features that was further revised through conducting graph-edits for final representation.

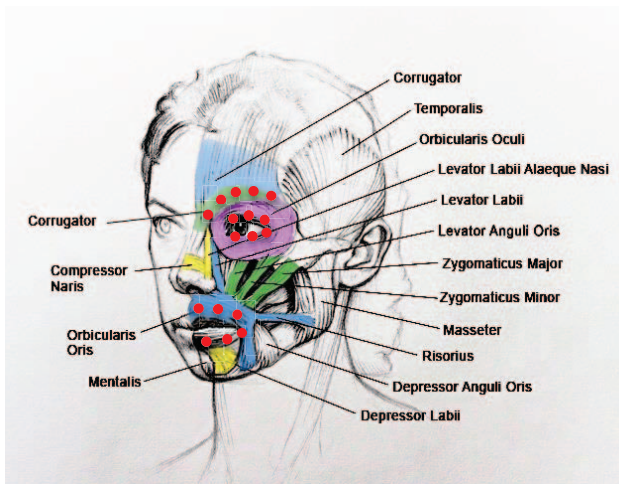


Fig. 5 Facial expression muscle anatomy and related landmarks (Mohseni et al. 2014).

Furthermore, some current methods exploit landmark selection to avoid the information that is not related to facial affects. Landmarks locating external contour and nose are frequently discarded (Mohseni et al. 2014; Dapogny et al. 2018) (see Figs. 6a, 6b). Sechkova et al. (2016) and Zhong et al. (2019) chose to remove the landmarks of the facial outline and applied a small window around each remaining landmark as one graph node, while the local features were extracted by Scale Invariant Feature Transform (*SIFT*) (Lowe 2004) and *Gabor* filter (Liu and Wechsler 2003) respectively. As mentioned at the beginning, since these local patches were segmented to introduce facial appearance into the graph representation rather than as independent nodes, similar to (Liu et al. 2019), we still classify them in landmark-level graphs. For a more extreme instance, Lei et al. (2020) only used 28 landmarks of the eyebrows and mouth areas that had significant contributions to micro-expressions. By doing this, it could increase attention to muscle movements that might occur during displaying a facial affect. On the other hand, in order to build more comprehensive graph representations, strategies based on FACS have been designed to select reasonable landmarks. Hassan and Mohammed (2020) picked out landmarks that indicated both ends of eyebrows, eyes, nose, mouth, upper and lower lips, plus two points on each side of the face contour (in total 20 landmarks). Then the generated facial graph could keep an appropriate dimension and represent sufficient affective information.

In addition, edges are another key element that cannot be ignored in graph definition. For landmark-level graphs, a fully connected graph is the most intuitive way to form edges (Durmuşoğlu and Kahraman 2016; Buhari et al. 2020; Zhong et al. 2019; Hassan and Mo-

ammed 2020; Lei et al. 2020). However, the number of edges is $n(n-1)/2$ for a complete graph with n nodes, which means the complexity of the spatial relationship will increase as the number of nodes increases. This positive correlation is not so correct in analyzing facial affects. For example, assuming the left eyebrow has five landmarks (see Fig. 5), the edge connecting adjacent landmarks or landmarks at both ends is obviously helpful. By contrast, links between other non-adjacent nodes seem not that necessary. Since the various parts of the eyebrow mostly move in concert when displaying facial affects, the changing trends contained in these edges are redundant. To this end, researches like Tanchotsrinon et al. (2011) and Mohseni et al. (2014) manually reduced edges based on knowledge of muscle anatomy and FACS, with results of 21 edges of 14 landmarks and 53 edges of 50 landmarks respectively. Another type of approaches is to exploit triangulation algorithms (Sabzevari et al. 2010; Dapogny et al. 2018), such as *Delaunay* triangulation (Kakumanu and Bourbakis 2006), to generate edges of a facial graph. The triangular patches formed by landmarks are consistent with true facial muscle distribution and edges are uniform for different subjects (Liu et al. 2019). Similarly, the landmark-level graph representation with triangulation is also utilized in generating sparse or dense facial mesh for 3D FAA (Pei and Zha 2009; Kotsia and Pitas 2006). For edge attributes of these facial graphs, the *Euclidean* distance is the simplest and most dominant metric, even with multiple normalization methods including diagonal line (Tanchotsrinon et al. 2011), inner-eyes distance (Liu et al. 2019) and maximum distance (Hassan and Mohammed 2020). The gradient computation (Buhari et al. 2020) and hop distance (Zhou et al. 2020b) have also been explored as edge attributes to model spatial relationship in different levels. Apart from the above edge connection strategies, several learning-based edge generation methods (e.g., Bayesian method (Sabzevari et al. 2010), *LT* (Kaltwang et al. 2015), Conditional Random Field (Walecki et al. 2017)) have been proposed to automatically extract semantic information from facial graphs. This part is discussed in detail in Sec. 4.1 and 4.4.

3.1.2 Region-level graphs

Region-level representations usually describe faces in terms of individual local areas and thereby ignore the spatial relationships among facial components. To solve this shortcoming, using graph structure to encode the spatial relations into the region-level representation is intuitive. Although many graph-based representations can be constructed in a region-level manner, there are

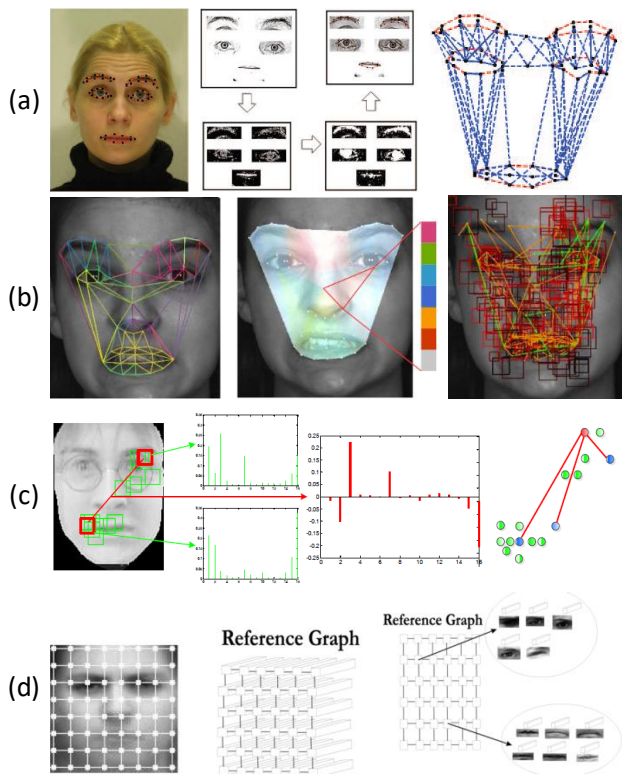


Fig. 6 Spatial graphs. (a) Landmark-level graph with FACS-based edges (Mohseni et al. 2014); (b) Landmark-level graph with automatic triangle edges (Dapogny et al. 2018); (c) ROI graph with edges computed based on correlation (Yao et al. 2015); (d) Patch graph with individual nodes (Zafeiriou and Pitas 2008).

two main categories of affective graphs: region of interest (ROI) graphs and patch graphs.

ROI graphs partition a set of facial areas as graph nodes which are highly related to affective display. Coordinates of facial landmarks are commonly applied to locate and segment ROIs. Unlike a few landmark-level graph representations that only use texture near all landmarks as supplementary information, ROI graphs explicitly select meaningful areas as graph nodes, and edges do not entirely depend on established landmark relationships. Zhang et al. (2020) built mappings between 24 ROIs and 12 AUs, and then selected representative landmarks that spotted ROI centers according to descriptions in FACS. Next, the authors introduced the idea of heatmap and employed the *HRNetV2* (Wang et al. 2020) as the backbone network to regress the ROI maps. Each spatial location in the extracted feature map were considered as one node of the facial graph, while edges were induced among node pairs. Similarly, Fan et al. (2020) predefined the central ROI locations based on facial landmarks and utilized feature maps of ROIs outputted by the *ResNet-50* (Xiao et al. 2018) as nodes to construct a K-Nearest-Neighbor (*KNN*)

graph. For each node, its pair-wise semantic similarities were calculated, and the nodes with the closest *Euclidean* distance were connected as initial edges. Another example is Liu et al. (2021), the authors employed the Main Directional Mean Optical-flow (*MDMO*) (Liu et al. 2015) as node attributes of 36 ROIs segmented based on 66 landmarks. And a *KNN* graph was generated in *MDMO* space to encode the local manifold structure for a sparse representation. Due to different AUs possibly occurring at the same location, Liu et al. (2020b) firstly defined 12 shared local ROIs and one global ROI by taking FACS and landmarks as reference. Subsequently, the *EAC-Net* (Li et al. 2017) was exploited to refine the location of ROIs, and each ROI was then fed into an Auto-Encoder (*AE*) to obtain its latent vector, which was regarded as the node attribute. In addition, the method of obtaining ROIs without relying on facial landmarks has also been studied. Yao et al. (2015) proposed a pair-wise learning strategy to automatically discover regions that were in part consistent with the locations of AUs (see Fig. 6c). The Local Binary Pattern (*LBP*) histograms (Zhao and Pietikainen 2007) of the learned facial regions and their feature correlations were taken as node and edge attributes of an undirected graph (either fully connected or highly sparse) respectively to construct two discriminative representations.

Different from ROI graph representations, the graph nodes in patch graphs are local areas evenly distributed or partitioned in a fully automatic manner from raw face images without manual prior guidance. Zafeiriou and Pitas (2008) created a reference bunch graph by evenly overlaying a rectangular graph on object images (see Fig. 6d). For each node of the graph, Normalized Morphological Multi-scale Analysis (*NMMA*) based on *Gabor* filters (Lyons et al. 2000) was designed to compute a set of feature vectors for different facial instances. The structure of the graph representation was optimized by solving an Elastic Graph Matching (*EGM*) problem which is discussed in Sec. 4.4. Such grid derived graph representation was also applied in Wu et al. (2019). Each pixel of the image was set as one node of an undirected graph, while every node was connected to pixels at a *Euclidean* distance below a certain threshold. Recently, several graph representations try to introduce regions beyond facial parts or single face image as context nodes. Zhang et al. (2019a) exploited the *RPN* (Ren et al. 2016) with a backbone of *VGG16* (Simonyan and Zisserman 2014) to extract feature vectors from 10 regions including both the target face and its contexts. The affective relationship between every two nodes was calculated based on the feature vectors to generate graph edges. Xie et al. (2020b)

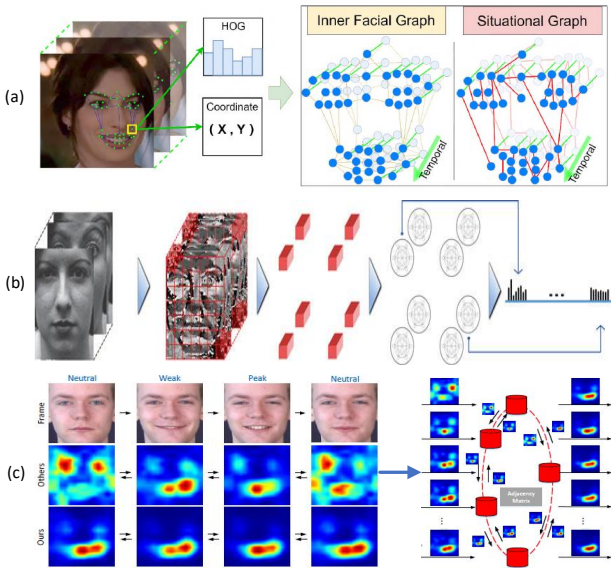


Fig. 7 Spatio-temporal graphs. (a) Landmark-level graph with adaptive edges (Zhou et al. 2020a); (b) Region-level graph with edges computed based on transitional masks (Rivera and Chae 2015); (c) Frame-level graph with learned edges (Liu et al. 2020a).

built two graph representations for cross-domain FAA. Holistic and local feature maps (eyes, nose, mouth corners) were firstly extracted from corresponding regions by *MTCNN* (Zhang et al. 2016) and *ResNet-50* (He et al. 2016) for both the source domain and the target domain. Then, three type of connections, global-to-global connection, global-to-local connection and local-to-local connection were computed according to statistical feature distribution acquired by *K-means* algorithm and fine-grained iterative update. They were further used to initialize the corresponding graph nodes and establish intra graph and inter graph respectively.

3.2 Spatio-Temporal Graph Representations

Literally, spatio-temporal representations deal with a sequence of frames within a temporal window, and can describe the dynamic evolution of facial affects, especially those subtle affective variations (e.g., eye blinking). In particular, introducing temporal information allows nodes in different static graphs to interact with each other, and generates a more complex graph representation of affective face. Figure 7 presents frameworks of different spatio-temporal graph representations.

Most existing approaches extend spatial graphs to the spatio-temporal domain. Rivera and Chae (2015) first chose a *Kirsch* compass mask (Kirsch 1971) to obtain the directional number response of each facial grid in eight different directions, while a 3D *Gaussian*-

like weighted compass mask gave nine space-time directional edge responses corresponding to each of the symmetry planes of a cube. The 2D and 3D masks provided facial information for a given local neighborhood, and were then used as nodes to define a spatio-temporal Directional Number Transitional Graph (*DNG*). Such weighted and directed graph could represent salient facial changes and statistic frequency of affective behaviors over time (see Fig. 7b). Several representations defining temporal connections between landmarks in adjacent frames have been proposed, which can be seen as landmark-level spatio-temporal graphs. Zhou et al. (2020b) developed a spatial temporal facial graph with selected facial landmarks attributed by *HOG* and *XY* coordinates as nodes. The intra-face edges were initialized based on semantic facial structure, while the inter-frame edges were created by linking the same node between consecutive frames. Similar landmark-based edge initialization in temporal domain was also utilized in Chen et al. (2019). In the extension (Zhou et al. 2020a), the authors introduced a connectivity inference block, called Situational Link Generation Module (*SLGM*), that could automatically generate dynamic edges to construct a spatio-temporal situational graph for a representation of part-occluded affective face (see Fig. 7a). Not like landmark-level graphs, Liu et al. (2020a) first extracted a holistic feature of each frame by *VGG16* and set them as individual nodes to establish a fully connected graph (see Fig. 7c). And the edge connections would be updated during learning long-term dependency of nodes in time series, which could be seen as a frame-level graph representation.

3.3 AU-level Graph Representations

Apart from using knowledge of AUs and FACS in the above two types of affective graphs, many graph representations have been proposed to model affective information from the perspective of AUs themselves. We divide these approaches into two categories: AU-label graph and AU-map graph. Figure 8 shows frameworks of different AU-level graph representations.

3.3.1 AU-label graphs

Different from spatial and spatio-temporal representations, AU-label graphs concentrate on building an affective graph from the label distribution of training data. Tong et al. (2007) computed the co-occurrence and co-absence dependency between every two AUs from existing facial affect database (see Fig. 8a). Since the dependency of any two AUs is not always symmetric, these relationships of AU labels were used as edges to construct

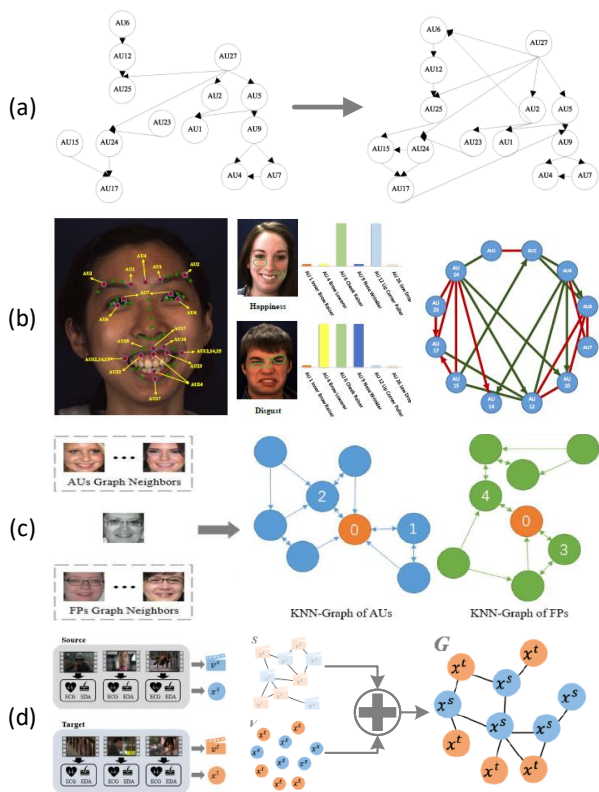


Fig. 8 AU-level and Other graphs. (a) AU-label graph with edges generated from training data (Tong et al. 2007); (b) AU-map graph with FACS based edges (Li et al. 2019b); (c) Auxiliary graphs of both AUs and landmarks (Chen et al. 2020); (d) Multi-modal graph of both visual and physiological signals (Chien et al. 2020).

an initial Directed Acyclic Graph (*DAG*). Similarly, Zhu et al. (2014) followed the definition of *DAG* and maximized the Bayesian Information Criterion (*BIC*) score function to learn the graph structure. In Lo et al. (2020), an AU-label graph was built with a data-driven asymmetrical adjacency matrix that denoted the conditional probability of co-occurrence AU pairs. The initial dependent representation of each AU would be set as learnable weights of the spatio-temporal features outputted by a *3D-ResNet-18* (Tran et al. 2018) to generate ultimate predictions. On the other hand, Cui et al. (2020) established a *DAG* where object-level labels (facial affect category) and property-level labels (AU) were regarded as parent nodes and child nodes respectively. The conditional probability distribution of each node to its parents was measured to obtain graph edges for correcting existing labels and generating unknown labels in large-scale FAA databases.

3.3.2 AU-map graphs

Judging from the elements used in a graph construction, AU-map graphs are very close to some region-level spa-

tial representations, because they all employ regional features as the attribute of graph nodes. But AU-map graphs further extract the feature maps that represent corresponding AUs. Similar to ROI graphs, Li et al. (2019b) first extracted a multi-scale global appearance feature with *VGG19* (Simonyan and Zisserman 2014) and cropped it into several ROI regions based on landmark locations to learn 12 AU features. These learned AU features and the AU relationships gathered from both training data and manually pre-defined edge connections (Tian et al. 2001) were combined to construct a knowledge graph (see Fig. 8b). The homologous protocol was also conducted in Xie et al. (2020a) and Zhou et al. (2020c), the former utilized *STPNet* (Qiu et al. 2017) followed by global average pooling to obtain corresponding AU features of graph nodes, while a *Dual-Inception* (Zhou et al. 2019) network with *optical-flow* images as input was exploited in the latter. Some special AU-map graphs have been proposed to introduce structure learning for more complex FAA tasks. Walecki et al. (2017) trained a Convolutional Neural Network (*CNN*) to jointly learn deep facial features from multiple databases. And these corresponding individual AU features were then used to represent graph nodes. The *copula functions* (Berkes et al. 2008) was applied to model pair-wise AU dependencies in a Conditional Random Field (*CRF*) graph. To account for indistinguishable affective faces, Corneanu et al. (2018) designed a *VGG*-like patch prediction module plus a fusion module to predict the probability of each AU. A prior knowledge taken from the given databases and a mutual gating strategy were used simultaneously to generate initial edge connections. In order to model uncertainty of AUs in real world, Song et al. (2021) established an uncertain graph, in which a weighted probabilistic mask that followed *Gaussian* distribution was imposed on each AU feature map extracted by *ResNet18* (He et al. 2016). By doing this, both the importance of edges and the underlying uncertain information could be encoded in the graph representation.

3.3.3 Other AU-level graphs

A few approaches of building AU-level graph representations from other aspects have been studied. Niu et al. (2019) proposed two Deep Neural Networks (*DNNs*) to extract multi-view AU features for both labeled and unlabeled face images. The parameters of these two *DNNs* were used as graph nodes to share the latent relationships among individual AUs which were embedded in the AU classifier to assist the semi-supervised AU recognition. Chen et al. (2020) established two *KNN* graphs of facial landmarks and AUs separately by using their

deep features extracted from the training data. The indexes of both central image and its neighbors were stored in an index-similarity list to boost the Label Distribution Learning (*LBL*). The generated auxiliary label space graphs followed an assumption that facial images should have nearby distributions to their neighbors in the label space of auxiliary tasks (see Fig. 8c). It was similar to the idea of Cui et al. (2020).

3.4 Other Graph Representations

Recently, several graph representations that do not fall into the above categories have been proposed, which indicates that this is still an open research field. In order to combine signals from multiple corpus, Chien et al. (2020) proposed a dual-branch framework, in which the visual semantic features were extracted by a *3D-CNN* (Hara et al. 2018) in both source and target sets. These features were then retrieved with *Spearman* correlation coefficient to generate positive edge connections in the manner of cross corpus (see Fig. 8d). Such learnable visual semantic graph could be used to perform training and prediction by masking nodes of different induced Low-level Physiological Descriptor (*LLD*) sets respectively. Xu et al. (2020b) built an emotion-based directed graph according to label distributions of facial affects in existing training data. Specifically, its nodes were initialized word vectors of the corresponding emotions, while the edges represented conditional probabilities of pair-wise emotions. The learned local relationship patterns could be injected into a network at the feature level to enhance the performance of final multimedia affect tagging.

Besides, some special graph representations of FAA such as Spectral Graph Transform (*SGT*) (Zheng et al. 2006; Derkach and Sukno 2017; Meena et al. 2018) and Non-negative Matrix Factorization (*NMF*) (Zhi et al. 2010; Kung et al. 2015) have also been explored.

3.5 Discussion

As an important part of graph-based FAA, there is a certain causal relationship between the choice of graph representation methods and the selection of relational reasoning methods. The spatio-temporal graph and the AU-level graph are most notable recent trend of graph-based facial representations. And the limitations of the three types are discussed as follows.

Spatial graph: Conceptually, landmark-level graphs have certain limitations from both externally and internally. On one hand, most of the generated graphs are sensitive to detection errors of facial landmarks,

thereby may fail in uncontrolled conditions. On the other hand, the selection of landmarks and the connection of edges have not yet formed a standard rule. Although some FACS-based strategies have been designed, the effects of different landmark sets and different edge connections on the graph representation are rarely reported. Finally, recent trend of developing FAA methods is to combine every procedure as an end-to-end learning pipeline. Thus, how to integrate the process of establishing landmark-level graphs into existing frameworks still needs to be studied.

Comparing with landmark-level graphs by modeling the facial shape variations of fiducial points, region-level graph representations explicitly encode the appearance information in local areas. And the spatial relationships among selected regions are measured through feature similarity instead of manual initialization based on facial geometry. The graph reasoning will be the next step to learn task-specific edge connections and discriminative affective features using techniques such as *CNNs* (Luo et al. 2017) or *GNNs* (Li and Gupta 2018), which are discussed in Sec. 4. The two types of region-level graph representations have their own characteristics, but have some flaws as well. For the ROI graphs, the circumstance resulting from inaccurate or unreasonable landmarks will also have an impact on some related representations. In addition, the contribution of geometric information for FAA has been proven in Zhang et al. (2017), thereby should be more effectively integrated into ROI graph representations. For patch graphs, incorporating context regions or multiple face regions into graph nodes is an emerging topic. Due to that most existing approaches utilize a region searching strategy, the problem is how to avoid the loss of target face and how to exclude invalid regions. Besides, as far as the literature we have collected, there is no work on combining the ROI graph and patch graph to construct a joint graph representation, which we think is a promising direction.

Spatio-temporal graph: Despite the advantage of extra dynamic affective information in spatio-temporal graphs, there are several drawbacks in existing methods. For landmark-level graphs, the current initialization strategy of edge connections is simply to link the facial landmark with the same index frame by frame. No research has been reported to learn the interaction of landmarks with different indexes in the temporal dimension. Besides, in addition to *Euclidean* distance and *Hop* distance, other edge attributes measurement methods should also be explored to model the semantic context both spatially and temporally. For the frame-level graph, the domain knowledge related to affective behaviors like muscular activity that can be embedded

with graph structure is not explicitly considered in recent work. Therefore, building a hybrid spatio-temporal graph is a practical way to encode the two levels of affective information at the same time.

AU-level graph: Most AU-label graphs rely on the label distributions of one or multiple given databases. One problem is the available AU labels because not every public database provides the annotated AU label. In addition, since AU labeling requires annotators with professional certificates and is a time-consuming task, existing databases with AU annotations are usually small-scale. Therefore, the distribution from limited samples may not reflect the true dependencies of individual AUs. To address this demand, some semi-supervised methods are introduced based on underlying assumptions like the potential mapping between facial affect categories and AUs. However, the reliability of this hypothesis is questionable when faced with complex FAA tasks including micro-expression recognition and continuous affect prediction. Another problem is that the measurement criteria of AU correlations are versatile but not general for both AU-label graphs and AU-map graphs, and can result in different initialized AU dependencies. The impact of these measurements on FAA still needs to be evaluated.

4 Affective Graph Relational Reasoning

The relational reasoning is the other significant procedure for graph-based FAA methods. The ability to reason about the relations between entities and their properties is believed to be the crucial step towards actual intelligence for machine learning systems (Kemp and Tenenbaum 2008). Such a mechanism can be considered as a two-step process, i.e., understanding the structure from a certain group of entities and making inference of the system as a whole or the property within. Consequently, a model that is able to perform relational reasoning has to output the structure as well as the property of the unstructured entity set. However, things are slightly different in the case of graph-based FAA. Depending on what kind of affective graph representation is exploited, the contribution of graph relational reasoning can be either merged before the decision level with other affective features, or reflected as a collaborative way in the level of feature learning. In this Section, we review relational reasoning methods designed for affective graph representations in four categories: dynamic Bayesian networks, classical deep models, graph neural networks and other traditional machine learning techniques.

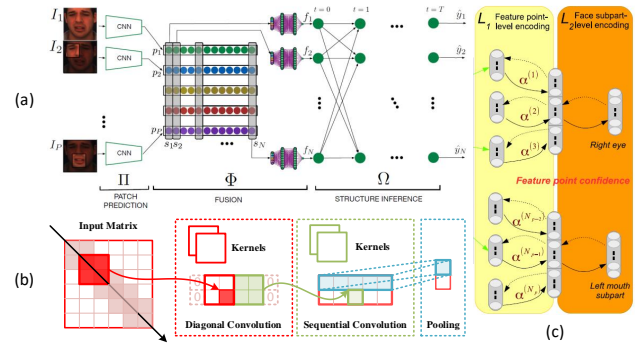


Fig. 9 Classical deep models for relational reasoning. (a) RNN (Corneanu et al. 2018); (b) CNN (Liu et al. 2019); (c) AE (Dapogny et al. 2018).

4.1 Dynamic Bayesian Network

Dynamic Bayesian Networks (DBNs) are models used to capture relationships mostly in AU-label graph representations. The Bayesian network is a DAG that reflects a joint probability distribution among a set of variables. In this DAG, the nodes indicate variables and the edges represent the conditional dependency among variables. In the work of Tong et al. (2007), a DAG was manually initialized according to prior knowledge, then larger databases were used to perform structure learning to find the optimal probability graph structure. After that, the probabilities of different AUs were inferred by learning the DBN. Following this idea, Zhu et al. (2014) additionally integrated DBN to a multi-task feature learning framework and made the AU inference by calculating the joint probability of each category node. Another advanced research of DBN is Cui et al. (2020). The inherent relationships between category labels and property labels were modelled by a DBN. And the DBN parameters were utilized to denote the conditional probability distribution of each AU given the facial affect. The wrong labels could be corrected by leveraging the dependencies after the structure optimization.

4.2 Adjustments of Classical Deep Model

Before GNNs are widely employed, many studies have adopted conventional deep models to process affective representations with the graph structure. These deep models are not specifically designed but is able to conduct standard operations on graph structural data by adjusting the internal architecture or applying additional transformation to the input graph representation. Figure 9 shows examples of classical deep models for graph learning.

4.2.1 Recurrent neural network

The variant of Recurrent Neural Networks (*RNNs*) is one of the successful extended model types for handling graph structural inputs. Similar to random walk, [Zhong et al. \(2019\)](#) applied a Bidirectional Recurrent Neural Network (*BRNN*) to deal with its landmark-level spatial graph representation in a rigid order. To incorporate the structural information represented by *Euclidean* distance, the extracted *Gabor* feature of each node in the graph was updated by multiplying with the average of the connected edges. Subsequently, the nodes were iterated by a *BRNN* with learnable parameters in both the forward and the backward direction. And the outputs were further fed to a fully-connected (*FC*) layer and a *softmax* layer for facial affect classification. In the work of [Corneanu et al. \(2018\)](#), the authors built a structure inference module to capture AU relationships from an AU-map graph representation. Based on a collection of interconnected recurrent structure inference units and a parameter sharing *RNN*, the mutual relationship between two nodes could be updated by replicating an iterative message passing mechanism with the control of a gating strategy (see Fig. 9a). And the final messages and previous individual AU estimations were combined to produce advanced AU predictions.

4.2.2 Convolutional neural network

Different from the sequential networks, [Liu et al. \(2019\)](#) utilized a variant *CNN* to process the landmark-level spatial affective graph. Compared to standard convolution architectures, the convolution layer in this study convolved over the diagonal of a special adjacency matrix so that the information can be aggregated from multiple nodes. Then a list of the diagonal convolution outputs were further processed by three sequential convolution layers which were 1-D convolutions. The corresponding pooling processes were performed behind convolution operations to integrate feature sets (see Fig. 9b). Predictions of facial affects were outputted by *FC* and *softmax* layers. Another attempt for landmark-level spatial graph representations is the *Graph-TCN* ([Lei et al. 2020](#)). It followed the idea of *TCN* residual blocks that consisted of standard convolution, dilated casual convolution and weight normalization ([Bai et al. 2018](#)). By using different dilation factors, *TCNs* were applied to convolve the elements that are both inside one node sequence and from multiple node sequences. Thus, the *TCN* for a node and *TCN* for an edge could be trained respectively to extract node feature and edge feature at the same time. Besides, [Fan et al. \(2020\)](#) exploited a Semantic Correspondence Convolution (*SCC*) module

to model the correlation among its region-level spatial graph. Based on an assumption that the channels of co-occurrence AUs might be activated simultaneously, the Dynamic Graph Convolutional Neural Network (*DG-CNN*) ([Wang et al. 2019](#)) was applied on the edges of the constructed *KNN* graph to connect feature maps sharing similar visual patterns. After the aggregation function, affective features were obtained to estimate AU intensities.

4.2.3 Auto-Encoder network

The approach of *AEs* has also been explored. [Dapogny et al. \(2018\)](#) employed a hierarchical auto-encoder network to capture the relationship from the constructed landmark-level spatial graph. Specifically, the first stage learned the texture variations based on the extracted *HOG* features for each node. While the second stage accumulated features of multiple nodes whose appearance changes were closely related and computed the confidence scores as the triangle-wise weights over edges (see Fig. 9c). Finally, a Random Forest (*RF*) was used for facial affect classification and AU detection simultaneously.

4.3 Graph Neural Network

Not like conventional deep learning frameworks mentioned in Sec. 4.2, *GNNs* are proposed to extend the 'depth' from 2D image to graph structure and established an end-to-end learning framework instead of additional architecture adjustment or data transformation. Several types of *GNNs* have been successfully used to address the relational reasoning of affective graph representations in FAA methods. Figure 10 illustrates several *GNN* architectures for relational reasoning.

4.3.1 Graph convolutional network

Graph Convolutional Networks (*GCNs*), especially the spatial *GCN* ([Kipf and Welling 2017](#)), are the most popular *GNN* in graph-based FAA research. Practically, *GCNs* can be set as an auxiliary module or part of the collaborative feature learning framework. For the former, *GCNs* are applied immediately after the graph representation. However, the outputs of relational reasoning are not directly used for facial affect classification or AU detection, but are later combined with other deep features as a weighting factor. In *MER-GCN* ([Lo et al. 2020](#)), the AU relationships were modelled by the conditional probability in an AU-label graph representation. Each node was represented as a one-hot vector

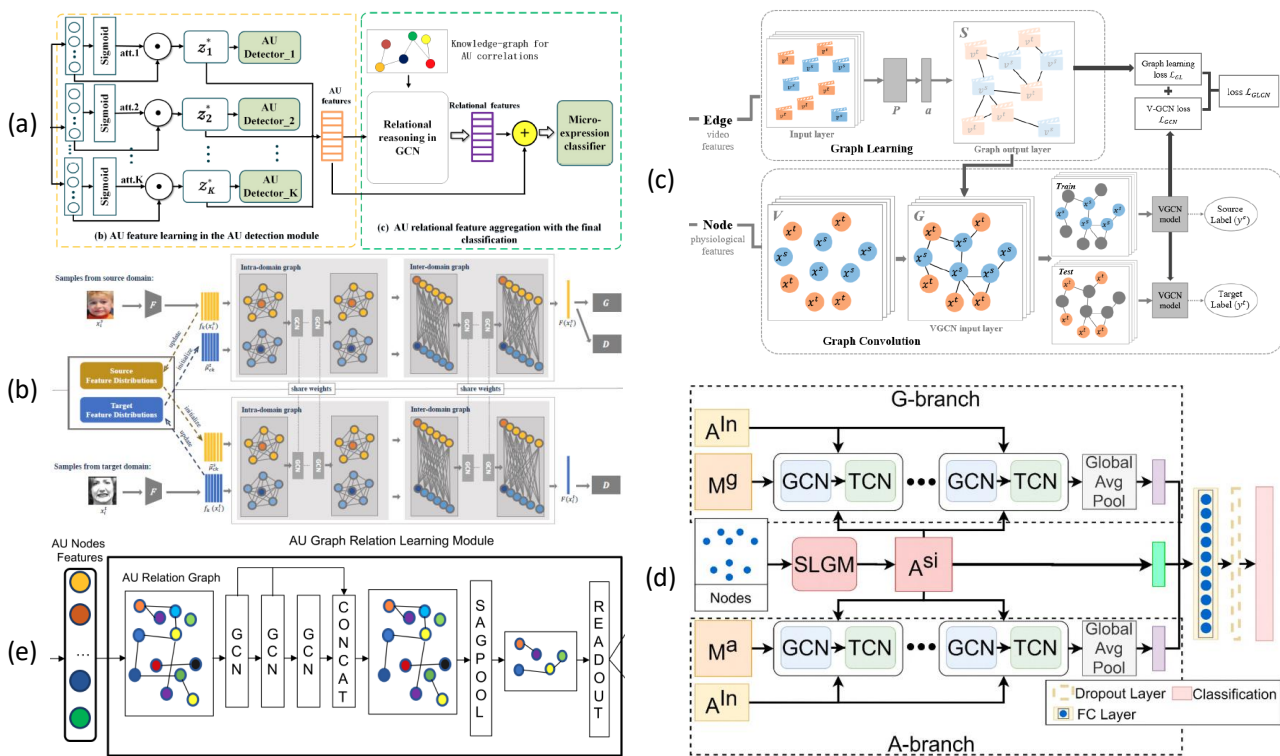


Fig. 10 Graph neural networks for relational reasoning. (a) GCN as auxiliary module (Zhou et al. 2020c); (b) GCN for atypical graph representation (Xie et al. 2020b); (c) GCN as collaborative framework (Chien et al. 2020); (d) GCN for spatio-temporal graph representation (Zhou et al. 2020a); (e) GAT (Xie et al. 2020a).

and fed into a *GCN* to perform node dependency learning. The generated graph features were embedded to the sequence level deep feature together for final classification. Similarly, Niu et al. (2019) employed a two-layer *GCN* for message passing among different nodes in its AU-level graph. Both the dependency of positive and negative samples were considered and used to infer a link condition between any two nodes. And the output of *GCN* was formulated as a weight matrix of the pre-trained AU classifiers. Zhou et al. (2020c) performed relational reasoning with *GCN* that provided an updated relational graph feature for each graph node by aggregating features from all neighbors based on edge weights (see Fig. 10a). Besides, *GCNs* can also be utilized following the above manner to execute relational reasoning on atypical graph representations, such as multi-target graph (Zhang et al. 2019a), cross-domain graph (Xie et al. 2020b) (see Fig. 10b) and distribution graph (He and Jin 2019).

For the collaborative framework, *GCNs* usually inherit the previous node feature learning model in a progressive manner. Like in Liu et al. (2020b), a *GCN*-based multi-label encoder was proposed to update features of each node over a region-level spatial graph representation. And the reasoning process was the same as that in the auxiliary framework. Similar studies also

include Zhang et al. (2020) and Chien et al. (2020) (see Fig. 10c). In addition, to incorporate the dynamic in spatio-temporal graphs, Liu et al. (2020a) set *GCNs* as an imitation of attention mechanism or weighting mechanism to share the most contributing features to explore the dependencies among frames. After training, the structure helped nodes update features based on messages from the peak frame and emphasize the concerned facial region. A more feasible way is to apply *STGCN* (Li et al. 2019a) on spatial-temporal graphs (Zhou et al. 2020b; Chen et al. 2019). In their relational reasoning, features of each node were generated with its neighbor nodes in current frame and consecutive frames by using spatial graph convolution and temporal convolution respectively. To make inference of the node relation in a more dynamic manner instead of using a constant graph structure, Zhou et al. (2020a) proposed an additional module to adaptively generate conditional edges. Based on the spatio-temporal graph representation, the authors introduced a situational graph generation block that predicted the probability of a link between any two nodes (see Fig. 10d). This block was trained by the mean-square loss over the actual change degree of each link, so that the additional connections reflected the categorical information and were closed to the actual facial variations.

Alternatively, the approach of spectral *GCN* (Deferrard et al. 2016) has also been studied. Wu et al. (2019) performed the relational reasoning on a patch-level spatial graph representation by using graph convolutions in frequency domain. Each *GCN* block contained a graph signal filtering layer and a graph coarsening layer. Every two matched nodes were merged into a new node, and the weight of the new node was the sum of the weights of two matched nodes. By repeating this operation several times, one *FC* layer and one *softmax* layer were added for facial affect classification.

4.3.2 Graph attention network

Graph Attention Networks (*GATs*) aim to strengthen the node connections with high contribution and offer a more flexible way to process the graph structure (Veličković et al. 2017). Song et al. (2021) introduced an uncertain graph neural network with *GAT* as the backbone. For its AU-map graph representation, a symmetric weighted mask was employed to characterize the strength of links through parameters update during network training, with an aim to select the useful edges and depress the noisy edges and learn the AU dependencies in the graph for each node. In addition, the underlying uncertainties were considered in a probabilistic way, close to the idea of Bayesian methods in *GNN* (Zhang et al. 2019b), to alleviate the data imbalance by weighting the loss function. Different from directly applying *GAT* to achieve the attention, Xie et al. (2020a) proposed a graph attention convolutional network that added a self-attention graph pooling layer after concatenating three sequential *GCN* layers (see Fig. 10e). This improved the reasoning process on an AU-map graph representation, because only important nodes would be left and the aggregated node features contained contributions of both AU information and facial topology.

4.3.3 Other graph network

According to the structured knowledge graph organized from the AU-map representation, Li et al. (2019b) exploited a Gated Graph Neural Network (*GGNN*) (Li et al. 2016) to propagate node information. Similar to *RNNs*, it calculated the hidden state of next time-step by jointly considering the current hidden state of each node and its adjacent node. The relational reasoning could be done through the iterative update of *GGNN* over the graph representation. And the *GGNN* module was further integrated into a multi-scale *CNN* to embed the globally structured relationships between AUs in an end-to-end framework.

4.4 Traditional Machine Learning Model

Although refined deep features extracted by parameterized neural networks and gradient-based methods is the current mainstream, they require a large amount of training samples for effective learning. Due to the insufficient data in early years or the purpose of efficient computation, many non-deep machine learning techniques have been applied for affective graph relational reasoning. Graph structure learning is one of widely used approaches. In Kaltwang et al. (2015), the reasoning of its spatial graph representation was conducted by *LT* learning. Parameters update and graph-edit of *LT* structure were performed iteratively to maximize the marginal *log*-likelihood of a set of training data. Walecki et al. (2017) employed *CRF* to infer AU dependencies in an AU-map graph. The use of *copula* functions allowed it to easily model non-linear dependencies among nodes, while an iterative balanced batch learning strategy was introduced to optimize the most representative graph structure by updating each set of parameters with batches. Approaches of graph feature selection are also exploited in this part, including Correlation-based Feature Selection (*CFS*) (Durmuşoğlu and Kahraman 2016), graph embedding (Sechkova et al. 2016), graph sparse coding (Liu et al. 2021) and frequent sub-graphs mining (Hassan and Mohammed 2020). These methods have provided a more diverse concept for graph relational reasoning.

4.5 Discussion

The relational reasoning is a significant characteristic of graph-based methods compared to other FAA systems. Although different approaches can be exploited to achieve this purpose, drawbacks of the aforementioned four types are discussed as follows.

Dynamic Bayesian network: The vast majority of AU-label graph representations employ *DBNs* as their relational reasoning model. However, the representation quality highly relies on the available training data that need balanced label distribution in both positive-negative samples and categories. This strong assumption will limit the effectiveness of node dependencies learned by *DBNs*. While the work about correcting and generating labels based on *DBN* (Cui et al. 2020) has been proposed, current study has revealed the potential of *GCNs* in processing AU-label graphs. Another problem is that *DBNs* can only be combined with facial features as a relative independent module, and are hard to integrate into an end-to-end learning framework.

Classical deep model: Standard deep models, including *CNNs*, *RNNs* and *AEs*, have been explored to con-

duct graph relational reasoning before the emergence of *GNNs*. Even if they are suitable for more graph representations than *DBNs*, the required additional adjustments in input format or/and network architecture make the implementation inelegant. For example, the modification of convolutions in Liu et al. (2019) resulted in losses of node information, while the *RNNs* let node messages only be passed and updated in a specific sequence that suppressed the graph structure (Liu et al. 2020a). Besides, applying grid models cannot make full use of the advantage of graph. They focus more on local features of the input, but the global property represented by the graph is also very important for the analysis of facial affects. Thus, we think the specific designed networks like *GNNs* will become dominant in this part.

Graph neural network: *GNNs* are developing techniques in relational reasoning. Architectures with different focuses have been proposed, but have their shortcomings as well. For instance, *GCNs* cannot handle directed edges well (e.g., AU-level graphs), while *GATs* only use the node links without the consideration of edge attributes (e.g., spatial graphs). Besides, due to the low dimension of the nodes in affective graphs, too deep *GNNs* may be counterproductive. In addition, being an auxiliary block or part of the whole framework will influence the construction of *GNNs*. Therefore, how to manage graph representation and relational reasoning using *GNNs* still needs to be explored.

Traditional methods: Traditional machine learning models have taken a place in early studies. In fact, advanced techniques like *DBNs* and *GNNs* are partly inspired by them. Nevertheless, one of the reasons they have been replaced is that these approaches need to be designed separately to cope with different graph representations, similar to hand-crafted feature extraction. Hence, it is difficult to form a general framework. On the other hand, larger amounts of training data and richer computing resources allow deep models to perform more effective and higher-order relational reasoning on affective graphs.

5 Databases and Validation

5.1 Databases

Public databases of facial affect are applied as validation material in most FAA studies. Since details of existing databases are different in terms of scales, annotations, sample properties and so on, it provides another perspective to understand current trends of FAA. In this section, we present a comprehensive overview of commonly used databases including latest released ones

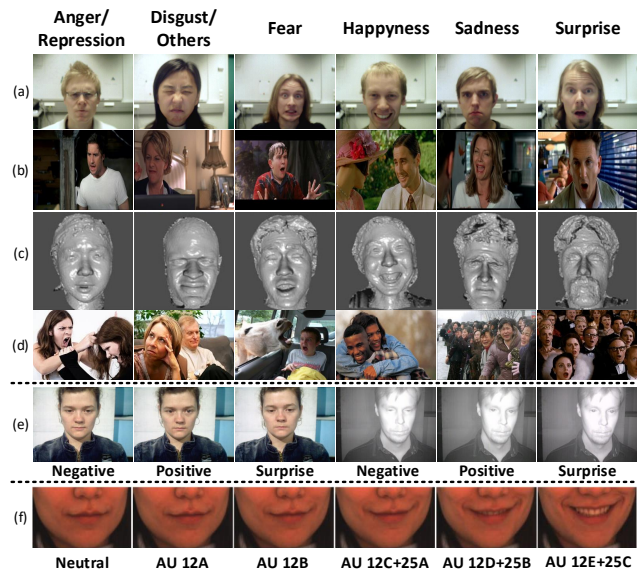


Fig. 11 Facial affect databases. (a) Oulu-CASIA contains posed facial affects; (b) SFEW 2.0 has facial affects under in-the-wild scenarios; (c) BP4D provides 3D affective face images; (d) EMOTIC, multiple faces appear in one image with V-A annotations; (e) The SMIC collects images of spontaneous micro facial affects in both visual light and near infrared light; (f) DISFA offers frame-level AU intensity labels.

that have larger data scale and more challenging factors. In addition, with an aim to emphasize the graph-based FAA, we summarize corresponding elements (e.g., landmark coordinates, AU labels) self-carried by databases, which are rarely considered in previous related surveys. In Table 1, the characteristics of these databases are listed from four aspects: samples, attributes, graph-related properties and special contents. Figure 11 exhibits several examples of facial affects under different conditions.

Databases containing posed facial affects are chosen by early FAA methods for validation. The Cohn-Kanade Dataset (CK) (Kanade et al. 2000), Extended CK Dataset (CK+) (Lucey et al. 2010), M&M Initiative Facial Expression Database (MMI) (Valstar and Pantic 2010) and Oulu-CASIA NIR&VIS Facial Expression Database (Oulu-CASIA) (Zhao et al. 2011) are the mostly used. And they all provide affective sequences with temporal evolution that are possible to meet requirements of different graph-based representations. A limitation of these four databases is the lack of in-the-wild conditions, which is less challenging for state-of-the-art methods. Hence, more recent databases such as FER-2013 (Goodfellow et al. 2015) and Static Facial Expression in the Wild (SFEW) 2.0 (Dhall et al. 2015) tend to acquire more complex affective data from internet or existing digital sources like movies and interviews. Different from the above two databases only

Table 1 An Overview of Facial Affect Databases

Database 'year	Samples			Attributes			Graph-based Properties ⁴			Special Contents ⁵
	Data Type	Subjects	Number	Eli. & Sou. ¹	Affects ²	B.B. ³	LM	AU	Dynamic	
CK(+) '10	Sequences	97(123)	486(593)	P & Lab	6B+N(+C)	● ● ● + I	●	●	●	/
MMI '10	Images/Videos	75	740/2900	P & Lab	6B+N	○ ○ ●	●	●	● + V	Head pose
Oulu-CASIA '11	Sequences	80	2880	P & Lab	6B	● ○ ○	●	●	●	NIR
DISFA '13	Sequences	27	130,000	S & Lab	6B+N	● ● ● + I	●	●	● + F	/
FER-2013 '13	Sequences	/	35887	S & Web	6B+N	● ○ ○	○	○	○	Wild
SFEW 2.0 '15	Images	/	1766	S & Movie	6B+N	● ○ ○	○	○	○	Wild
AFEW 7.0 '17	Videos	/	1809	S & Movie	6B+N	● ● ○	●	●	●	Audio, Wild
BU-3DFE '06	Images	100	2500	P & Lab	6B+N	● ● ○	○	○	○	3D, Multi-view, I
BU-4DFE '08	Videos	101	606	P & Lab	6B+N	● ● ○	●	●	●	3D, Multi-view
BP4D '14	Videos	41	328	S & Lab	6B+E+P	● ● ●	●	●	● + F	3D, Head pose
SMIC '13	Sequences	16	164	S & Lab	3B [†] +N	● ○ ○	○	○	●	Micro., NIR
CASME II '14	Sequences	35	247	S & Lab	3B [‡] +R+O	● ○ ●	●	●	● + V	Micro.
SAMM '18	Sequences	32	159	S & Lab	6B+C	● ○ ●	●	●	● + V	Micro.
CAS(ME) ² '18	Sequences	22	300+57	S & Lab	3B [†] +O	● ○ ●	●	●	● + V	Macro. & Micro.
EmotioNet '16	Images	/	950,000	S & Web	6B+17Comp.	● ● ● + I	○	○	○	Wild
ExpW '18	Images	/	91,793	S & Web	6B+N	● ○ ○	○	○	○	Multi-sub., Wild
RAF-DB '19	Images	/	29672	S & Web	6B+N+11Comp.	● ● ○	○	○	○	Wild
AffectNet '19	Images	/	420,299	S & Web	6B+N+C+O	● ● ○	○	○	○	V&A, Wild
EMOTIC '19	Images	/	23,571	S & Web	6B+N+19Comp.	● ○ ○	○	○	○	V&A, Multi-sub., Wild

¹ Eli.: elicitation; Sou.: source; P: posed; S: spontaneous.

² 6B: 6 basic affects (happiness, sadness, fear, anger, disgust, surprise); N: neutral; C: contempt; E: embarrassment; P: pain; O: others; R: repression; 3B[†]: 3 basic affects (positive, negative, surprise); 3B[‡]: 3 basic affects (happiness, disgust, surprise); Comp.: compound affects.

³ B.B.: bounding boxes; LM: landmarks; ● = Yes, ○ = No.

⁴ I: intensity annotation; V: onset-apex-offset annotation; F: frame-level annotation.

⁵ NIR: near-infrared; Multi-sub.: multiple subjects in one image; Micro.: micro-expression; Macro.: macro-expression; Wild: in-the-wild scenario; V&A: valence and arousal.

providing static images, the Acted Facial Expression in the Wild (AFEW) 7.0 (Dhall et al. 2017) is a temporal version of SFEW with spontaneous facial affects in all kinds of conditions, which are exhibited by professional actors with emotional context. Moreover, AFEW is also a multi-modal database that provides audio affective data. As a standard database of EmotiW competition, the content of AFEW will be updated synchronously.

Some other databases focus more on affective intensity in addition to discrete facial affects. The Denver Intensity of Spontaneous Facial Action Database (DISFA) (Mavadati et al. 2013) contains manually frame-level AU annotations and intensity labels from 0 to 5 for each AU. The Binghamton University 3D Facial Expression Database (BU-3DFE) (Yin et al. 2006) annotates 6 basic affects with four levels of intensity and provides both 3D facial texture images and geometric shape models. The Binghamton University 4D Facial Expression Database (BU-4DFE) is a dynamic extension of BU-3DFE, which contains multi-view 3D faces but no intensity annotations. The focus on spontaneous affects is also presented in this part. The Binghamton-Pittsburgh 3D Dynamic Spontaneous Facial Expression Database (BP4D) (Zhang et al. 2014) has both 2D and 3D spatio-temporal videos with facial affects containing head poses. The ground-truth of each AU is annotated frame by frame for 6 basic and 2 non-basic facial affects.

Another type of databases is for micro-expressions. Different from conventional affective databases, 'reaction' is mainly applied to collect subtle facial changes. For instance, participants are required to keep a neutral face while watching videos associated with induction of specific affects (Zhao and Li 2019). Following this setting, the Spontaneous Micro Facial Expression Database (SMIC) (Li et al. 2013), the Improved Chinese Academy of Sciences Micro-Expression Database (CASME II) (Yan et al. 2014) and the Spontaneous Micro-Facial Movement Database (SAMM) (Davison et al. 2018) have been released for micro FAA. Also, the Chinese Academy of Sciences Macro-Expression and Micro-Expression Database (CAS(ME)²) is developed for both macro-expressions and micro-expressions (Qu et al. 2018). However, due to the time-consuming of data collection and annotation, samples in these micro affective databases are insufficient and distribution imbalanced, and only contain lab-controlled conditions.

Recently, several large-scale databases have been developed to provide sufficient data with spontaneous facial affects and in-the-wild conditions, especially for FAA methods using deep learning. The Real-World Affective Face Database (RAF-DB) (Li and Deng 2019) offers nearly 30,000 in-the-wild images with both basic affects and compound affects (e.g., happily surprise, sadly angry). The Large-Scale Face Expression in-the-Wild dataset (ExpW) (Zhang et al. 2018b) contains

91,793 manually annotated original (without size normalization) web images. It additionally provides a subset that has multi-subject conditions with interpersonal relation labels. Similar characteristics can be found in the EMOTIC (Kosti et al. 2019) which has 34,320 annotated faces in 23,571 images. Besides, it also has continuous labels (valence, arousal, dominance) and extra compound emotion classes. AffectNet (Mollahosseini et al. 2019) is the largest existing database with over one million images, while 450,000 of them are manually annotated. And this is currently the biggest large-scale database that provides continuous affective labels (V-A). To avoid time-consuming manual annotation, EmotioNet (Fabian Benitez-Quiroz et al. 2016) designed a real-time algorithm to achieve automatic annotation of AUs, AU intensities and affective categories for 950,000 Internet images. Although there is still a certain accuracy gap between manual labels and automatic labels, this is a potential way to efficiently acquire massive labelled affective data.

Through observing the development of facial affective databases, we can conclude an evolutionary FAA path from posed, constrained, and conventional view to spontaneous, uncontrolled, and non-basic view. With regard to graph-based FAA, it is available to find and select suitable databases with corresponding metadata, such as landmarks, AU labels and dynamics, for different graph representation purposes. However, existing databases also have some shortcomings. On one hand, no or not accurate enough AU annotations are provided by in-the-wild databases, which limits the role that AUs can play in FAA. On the other hand, there is still a blank in the field of dynamic large-scale affective database, so that it is hard to use temporal information to generate affective graph representation. Finally, instead of discrete categories, databases about natural and spontaneous facial affects in continuous domain need more attention.

5.2 Evaluation Principle

To fairly evaluate FAA methods on public databases, a few standard validation protocols should be followed. The k-fold subject independent cross validation is a widely adopted version. The k-fold crossing operation guarantees the balance of the evaluation result on one database, while the subject-independent rule keeps the testing set isolated during training. An extreme version is the leave-one-subject-out cross validation, which is usually used in small-scale samples such as micro-expression databases. As many databases (i.e., SFEW 2.0 and EmotioNet) provide official groups of training, validation and testing sets, the holdout validation is

also exploited especially in some FAA competitions like EmotiW and AVEC. Another generic protocol is cross database validation that aims to evaluate the FAA generalization when facing training and testing data from different databases respectively.

The unified metric is another important part of the fair evaluation. One simple but effective metric is average accuracy rate. The F1 score and the area under the receiver operating characteristic (ROC) curve (AUC) are also widely adopted. In addition, the Pearson correlation coefficient and the Intra-class correlation (ICC(3,1)) are two common continuous metrics. The former measures relative differences between target and prediction (similar metrics also include mean squared error (MSE) and mean absolute error (MAE)), while the ICC(3,1) is used in behavioral science to measure agreement between annotators (e.g., AU intensity labels).

Although there are standard validation protocols and unified metrics, the results of various FAA methods can be hardly compared directly due to the different experimental configurations in terms of preprocessing approaches or data grouping strategies. Therefore, benchmarks based on public databases need to be studied in the future.

6 Applications and Performance

According to different description models of facial affects, the FAA can be subdivided into multiple applications. Typical output of FAA systems is the label of a basic facial affect or AUs. Recent researches also extend the goal to predict micro-expression or affective intensity labels or continuous affects. In this section, we compare and discuss the graph-based FAA methods presented in this paper from three main application categories: facial expression recognition, AU detection, and micro-expression recognition. Some special studies outside these three will also be evaluated.

6.1 Facial Expression Recognition

Facial expression recognition (FER), or namely macro-expression recognition, has been working on the topic of basic facial affects classification. A certain trend of FER is that the research focus has shifted from the early posed facial affects in controlled conditions to the recent spontaneous facial affects in real scenarios. In other words, the recognition of the former is considered as a solved problem for FAA methods including graph-based FER, which can be corroborated from the results in Table 2. For example, the performance on

CK+ database is very close to 100% (Kotsia and Pitas 2006; Rivera and Chae 2015; Wu et al. 2019; Liu et al. 2020a).

From the view of the representation, spatial graphs and spatio-temporal graphs are dominant. The only exception is Chen et al. (2020) where the authors utilized the auxiliary label space graphs of the landmark detection and AU detection to approximately learn the label distribution of facial affects. For the two mainly used graph representations, hand-crafted features (e.g., *LBP* (Yao et al. 2015), *Gabor* (Zhong et al. 2019), *HOG* (Liu et al. 2019; Zhou et al. 2020b)) or deep-based features (e.g., *VGG* (Liu et al. 2020a), *ResNet* (Xie et al. 2020a)) are employed to enhance the node representation similar to many non-graph FER methods (Zhao and Pietikainen 2007; Zhang et al. 2017). For reasoning approaches, early studies prefer to capture the relations of an individual node from predefined graph structures using tracking strategies (Kotsia and Pitas 2006; Zafeiriou and Pitas 2008; Mohseni et al. 2014; Rivera and Chae 2015) or traditional machine learning models (e.g., *RF* (Dapogny et al. 2018), *BRNN* (Zhong et al. 2019), *CNN* (Liu et al. 2019)). In some of the latest work, *GCNs* become one of the mainstream choice and show state-of-the-art performances on both posed and in-the-wild databases. Another observation is that the framework of combining the spatio-temporal graph representation and *GNNs* is getting more attention in FER studies (Zhou et al. 2020b,a; Liu et al. 2020a).

Despite many graph-based studies have shown improvements in predicting facial affects, there are still some potential topics for FER. One thing is that the goal of existing methods stays on classifying basic facial affects. No study of using graph-based methods to recognize compound affects (or mixture affects), whose labels are provided by recent databases like RAF-DB and EmotioNet, is reported. One possible solution is to introduce AU-level graph representations that can describe fine-grained macro-expressions with closer inter-class distances. The other topic is effective graph-based representations due to the big gap between the performance of current methods and the acceptable result in practice when analyzing in-the-wild facial affects. In addition, since existing databases lack sufficient dynamic annotated samples, the evaluation of spatio-temporal graphs in large-scale conditions remains to be explored.

6.2 Action Unit Detection

The AU detection (AUD) facilitates a comprehensive analysis of the facial affect and is typically formulated as a multi-task problem that learns a two-class classification model for each AU. It can not only expand the

recognition categories of macro-expressions through the AU combination (Kaltwang et al. 2015), but also can be used as a pre-step to enhance the recognition of micro-expressions (Zhou et al. 2020c). Comparing with graph-based FER, the wide usage of graph structures has a longer history in AU detection (Martinez et al. 2017) and has played a more dominant role. Table 3 presents a summary of graph-based AU detection methods including the performance comparison.

Specifically, spatial graphs and AU-level graphs are equally popular in the representation part of AUD. An interesting observation is that, no matter landmark-level or region-level, all the spatial graphs constructed in the listed AUD methods employed facial landmarks (Kaltwang et al. 2015; Sechkova et al. 2016; Dapogny et al. 2018; Liu et al. 2020b; Fan et al. 2020; Liu et al. 2019; Zhang et al. 2020). The possible reason is that the landmark information is helpful and effective for locating the facial areas where AUs may occur. In this setting, their node representations are close to that in spatial graphs of FER methods, which usually combine geometric coordinates with appearance features (e.g., *SIFT* (Sechkova et al. 2016), *HOG* (Dapogny et al. 2018; Liu et al. 2019)). Although some AUD methods using AU-level graphs also exploited traditional features (e.g., *Gabor* (Tong et al. 2007; Zhu et al. 2014), *LBP* (Cui et al. 2020)) or deep features (e.g., *VGG* (Corneanu et al. 2018)) to introduce appearance information, their graph representations were basically initialized from the AU label distribution of the training set. This has led to the *DBN* model becoming a major approach in the relational reasoning stage (Tong et al. 2007; Zhu et al. 2014; Cui et al. 2020). Another similar trend to graph-based FER is that *GNNs* have been widely utilized to learn the latent dependency among individual AUs in recent studies, such as *GCN* (Niu et al. 2019; Liu et al. 2020b; Zhang et al. 2020; Zhou et al. 2020c), *GAT* (Song et al. 2021), *GGNN* (Li et al. 2019b) and *DG-CNN* (Fan et al. 2020). But the difference is that *FC* layers (Li et al. 2019b; Niu et al. 2019; Liu et al. 2020b, 2019) or regression models (Walecki et al. 2017; Fan et al. 2020; Zhang et al. 2020) are often applied for predicting labels instead of *Softmax* classifier (Zhou et al. 2020c; Song et al. 2021).

A special line of AUD research analyzes the facial affects by estimating the AU intensities, which could have greater information value in understanding complex affective states (Zhi et al. 2020). Even though a few attempts in estimating AU intensities based on graph structures have existed (Kaltwang et al. 2015; Corneanu et al. 2018; Fan et al. 2020), the study of using the latest spatio-temporal graph representations and *GNNs* has not been reported. Another big challenge in AUD is

Table 2 Performance summary of representative graph-based FER methods discussed in this Paper

References	Prep. ¹	Representation ²			Reasoning ³		Posed Database ⁴	Wild Database	Validation ⁵
	B.B./LM	Cat.	Node	Edge	Model	Classif.			
Kotsia and Pitas 2006	o 104	$S : \mathcal{L}$	C	Δ	-->	SVM	CK ar: 99.7%	/	LO CV
Zafeiriou and Pitas 2008	• /	$S : \mathcal{P}$	NM	L	-->	EGM	CK ar: 97.1%	/	LO CV
Tanchotsrinon et al. 2011	• 14	$S : \mathcal{L}$	C	M+E	/	MLP	CK ar: 95.24%	/	HO
Mohseni et al. 2014	o 50	$S : \mathcal{L}$	C	M+E	-->	Adabst	MMI ar: 87.7%	/	10F CV
Rivera and Chae 2015	• /	$ST : \mathcal{R}$	Histo.	DNG	-->	SVM	CK+ ar: 100%; MMI ar: 97.6%; Oulu ar: 98.4%	/	10F CV
Yao et al. 2015	• /	$S : \mathcal{R}$	LBP	L	/	SVM CNN	/	SFEW ar: 55.38%; AFEW ar: 53.80%;	HO
Durmuşoğlu and Kahraman 2016	• 18	$S : \mathcal{L}$	C	F+E	CFS	MLP	MUG ar: 91.22%	/	HO
Dapogny et al. 2018	• 49	$S : \mathcal{L}$	C+HOG	Δ	AE	RF	CK+ ar: 93.4%; BU-4DFE ar: 75.0%	SFEW ar: 37.1%	10F-SI CV HO
Zhong et al. 2019	• 46	$S : \mathcal{L}$	Gabor	F+E	BRNN	SoftMax	CK+ ar: 98.27%; MMI ar: 94.44%; Oulu ar: 93.06%	/	10F-SI CV
Wu et al. 2019	• /	$S : \mathcal{P}$	Pixel	E	GCN	SoftMax	CK+ ar: 99.78%; JAFEE ar: 94.44%	/	HO
Chen et al. 2020	• /	$AU : \mathcal{O}$	Φ	KNN	/	SoftMax	CK+ ar: 93.08%; MMI ar: 70.49%; Oulu ar: 63.85%	SFEW ar: 56.50%; RAF ar: 85.53%; AffNet: ar: 59.35%	CD
Liu et al. 2019	• 68	$S : \mathcal{L}$	C+HOG	Δ	CNN	SoftMax	CK+ ar: 97.67%; MMI ar: 80.11%	SFEW ar: 55.36%	10F-SI CV HO
Xie et al. 2020b	• /	$S : \mathcal{P}$	ResNet	K-means	GCN	SoftMax	CK+ ar: 85.27%; JAFEE ar: 61.50%	SFEW ar: 56.43%; FER2013 ar: 58.95%; ExpW ar: 68.50%	CD
Zhou et al. 2020b	• 34	$ST : \mathcal{L}$	C+HOG	M+H	GCN	SoftMax	CK+ ar: 98.63%; Oulu ar: 87.23%	/	10F-SI CV
Hassan and Mohammed 2020	o 20	$S : \mathcal{L}$	C	F+E	gSpan	MLP	CK+ ar: 98.63%; Oulu ar: 87.23%	/	HO
Liu et al. 2020a	• /	$ST : \mathcal{F}$	VGG	F	GCN	BiLSTM	CK+ ar: 99.54%; Oulu ar: 91.04%; MMI ar: 85.89%	/	10F-SI CV
Zhou et al. 2020a	• 44	$ST : \mathcal{L}$	C+HOG	L+H	GCN	SoftMax	CK+ ar: 98.92%; Oulu ar: 87.50%	AFEW ar: 45.12%	10F-SI CV HO

¹ Prep.: processing; B.B.: bounding boxes; • = Yes, o = No; LM: landmarks.² Cat.: category; $S/ST/AU$: {spatial; spatio-temporal; AU-level} representation; $\mathcal{L}/\mathcal{R}/\mathcal{P}/\mathcal{O}/\mathcal{F}$: {landmark; region; patch; other; frame}-level graph; C: landmark coordinates; Histo.: histograms; Φ : label distributions; Δ : triangulation; $L/M/F$: {learning; manual; full} connections; E: Euclidean distance; H: Hop distance.³ Classif.: classifier; -->: tracking; gSpan: graph mining.⁴ ar: average accuracy rate; MUG (Aifanti et al. 2010); JAFEE (Lyons et al. 1999).⁵ CV: cross validation; LO: leave-one-out; HO: holdout validation; 10F: 10-folds; SI: subject independent; CD: cross database validation.

insufficient and imbalanced samples. The recent graph-based methods using transfer learning (Niu et al. 2019; Cui et al. 2020) or uncertainty learning (Song et al. 2021) were proposed to address this problem. They showed an advantage of graph-based method in this topic and are helpful to implement AUD in large-scale unlabeled data.

6.3 Micro-Expression Recognition

Micro-expressions are fleeting and involuntary facial affects that people usually exhibit in high stake situations when attempting to conceal or mask their true feelings. The earliest well-known studies came from Haggard and

Isaacs (1966) as well as Ekman and Friesen (1969). Generally, a micro-expression only lasts from 1/25 to 1/2 seconds long and is too subtle and fleeting for an untrained person to perceive. Therefore, developing an automatic micro-expression recognition (MER) system is valuable in reading human hidden affective states. Besides the short duration, the characteristics of low intensity and localization also make it challenging.

To this end, graph-based MER methods have been designed to address the above challenges, and have become appealing in the past two years (Liu et al. 2021), especially in 2020 (Lo et al. 2020; Lei et al. 2020; Xie et al. 2020a; Buhari et al. 2020; Zhou et al. 2020c). Table 4 lists the reported performance of a few representa-

Table 3 Performance summary of representative graph-based AUD methods discussed in this Paper

References	Prep. ¹		Representation ²			Reasoning ³		Database ⁴	Validation ⁵
	B.B.	LM	Cat.	Node	Edge	Model	Output		
Tong et al. 2007	•	/	AU : \mathcal{B}	Gabor	Φ	DBN	Adabst	CK ar: 99.33%; MMI (CK) ar: 93.9%	LOSO CV CD
Zhu et al. 2014	•	49	AU : \mathcal{B}	C+Gabor	Φ	DBN	MPE	CK+ ar: 90.48%, f_1 : 0.7072; DISFA ar: 93.56%, f_1 : 0.7095	2F, 10F CV
Kaltwang et al. 2015	o	66	S : \mathcal{L}	C	L	LT		DISFA corr: 0.43, mse: 0.39, icc: 0.36	9F CV
Sechkova et al. 2016	o	49	S : \mathcal{L}	C+SIFT	L	Graph Emb.	SVM	CK+ ar: 92.7%	LOSO CV
Walecki et al. 2017	o	/	AU : \mathcal{M}	CNN	L	CRF	Ordi. Regr.	FERA2015 (Valstar et al. 2015) icc: 0.63, mae: 1.23; DISFA icc: 0.45, mae: 0.61	HO
Corneanu et al. 2018	•	/	AU : \mathcal{M}	VGG	Φ	RNN	Sigmoid	BP4D f_1 : 61.7%; DISFA f_1 : 56.7%	3F-SI CV
Dapogny et al. 2018	•	49	S : \mathcal{L}	C+HOG	Δ	AE	RF	CK+ auc: 95.3%, f_1 : 78.8%, nf_1 : 86.5%; BP4D: auc: 72.7%, f_1 : 55.7%, nf_1 : 63.6%; DISFA auc: 82.4%, f_1 : 49.1%	10F-SI CV
Li et al. 2019b	•	20	AU : \mathcal{M}	C+VGG	M+L	GGNN	FC	BP4D auc: 74.1%, f_1 : 62.9%; DISFA auc: 80.7%, f_1 : 55.9%	no report
Niu et al. 2019	•	/	AU : \mathcal{O}	W	Trans. K	GCN	FC	BP4D f_1 : 59.8%; EmotioNet f_1 : 68.1%	3F-SI CV HO
Liu et al. 2020b	•	19	S : \mathcal{R}	EAC-Net +AE	M	GCN	FC	BP4D auc: 87.3%, f_1 : 62.8%; DISFA auc: 74.6%, f_1 : 55.0%	3F-SI CV
Fan et al. 2020	•	20	S : \mathcal{R}	ResNet	KNN+E	DG-CNN	Htm. Regr.	BP4D icc: 0.72, mae: 0.58; DISFA icc: 0.47, mae: 0.20	3F-SI CV
Liu et al. 2019	•	68	S : \mathcal{L}	C+HOG	Δ	CNN	FC	CK+ auc: 92.9%	10F-SI CV
Zhang et al. 2020	•	18	S : \mathcal{R}	HRNetV2	L	GCN	Htm. Regr.	BP4D f_1 : 63.5%; DISFA f_1 : 62.0%	3F-SI CV
Zhou et al. 2020c	•	/	AU : \mathcal{M}	Optical-flow +Inception	L	GCN	Softmax	CASME II (SAMM) f_1 : 61.10%; SAMM (CASME II) f_1 : 57.22%	LOSO CV CD
Cui et al. 2020	o	51	AU : \mathcal{B}	LBP	Φ	DBN	LR/ CNN/ SVM	CK+ f_1 : 0.830; BP4D f_1 : 0.687; EmotionNet f_1 : 0.626; MMI (CK+) f_1 : 0.532	5F-SI CV CD
Song et al. 2021	•	/	AU : \mathcal{M}	ResNet	Rand. M	GAT	Softmax	BP4D ar: 78.2%, f_1 : 63.3%; DISFA ar: 93.4%, f_1 : 60.0%	3F-SI CV

¹ Prep.: processing; B.B.: bounding boxes; • = Yes, o = No; LM: landmarks.² Cat.: category; S/AU: {spatial; AU-level} representation; : L/R/B/M: {landmark; region; label; map}-level graph; C: landmark coordinates; Φ : label distributions; Δ : triangulation; L/M: {learning; manual} connections; E: Euclidean distance; Trans. K: transfer knowledge; Rand. M: random mask.³ Graph Emb.: graph embedding; Ordi. Regr.: ordinal regression; Htm. Regr.: heatmap regression.⁴ ar: average accuracy rate; f_1 : F1 score; nf_1 : F1-norm score; corr: Pearson correlation coefficient; mae: mean absolute error; mes: mean squared error; icc: intra-class correlation coefficient, ICC(3,1); auc: area under the receiver operating characteristic curve; DB1 (DB2): train on DB2, test on DB1.⁵ CV: cross validation; LOSO: leave-one-subject-out; (K)F: k-folds; SI: subject independent; HO: holdout validation; CD: cross database validation.

tive recent work of graph-based MER. In terms of representation types, these methods fall into the landmark-level spatial graph (Liu et al. 2021; Lei et al. 2020; Buhari et al. 2020) and the AU-level graph (Lo et al. 2020; Xie et al. 2020a; Zhou et al. 2020c). For the former, their idea is to use landmarks to locate and analyze specific facial areas to deal with the local response and the subtleness of micro-expressions. And for the latter, they aim to infer the AU relationship to improve the final performance. The difference in processing ideas is also reflected in the reasoning procedure. Approaches like *GraphSC* (Liu et al. 2021) and variant *CNN* (Lei et al. 2020) are exploited in the landmark-level graph to integrate the individual node feature representations. While the *GCN* is employed to learn an

optimal graph structure of the AU dependency knowledge from training data and make predictions. But one common thing is that almost all the methods except (Buhari et al. 2020) consider the local appearance in a spatio-temporal way by using *optical-flow* or *DNNs*.

A problem in graph-based MER is the lack of large-scale in-the-wild databases. The small sample size limits the AU-level graph representation that rely on initializing the AU relationship from the AU label distribution of the training set. And the lab-controlled data make it difficult to follow the trend in FER studies, which generalizes the graph-based FAA methods in real-world scenarios. However, the analysis of uncontrolled micro-expressions is very important, because micro-expressions and macro-expressions can occur si-

Table 4 Performance summary of representative graph-based MER methods discussed in this Paper

References	Prep. ¹		Representation ²			Reasoning ³		Database ⁴	Validation ⁵
	B.B.	LM	Cat.	Node	Edge	Model	Classif.		
Lo et al. 2020	•	/	$AU : B$	Φ	KNN	GCN	$Softmax$	CASME II (7 cl.) ar : 42.71%	LOSO CV
Lei et al. 2020	•	28	$S : L$	TCN	F	$G-TCN$	$Softmax$	CASME II ar : 73.98%, f_1 : 72.46%; SAMM (5 cl.) ar : 75.00%, f_1 : 69.85%; SAMM (4 cl.) ar : 80.50%, f_1 : 76.57%	LOSO CV
Xie et al. 2020a	•	/	$AU : M$	$3DCNN$	L	GCN	$Softmax$	CASME II ar : 0.712, f_1 : 0.355; CASME II (7 cl.) ar : 0.561, f_1 : 0.394; SAMM (3 cl.) ar : 0.702, f_1 : 0.433; SAMM ar : 0.523, f_1 : 0.357 SMIC (CASME II): ar : 0.344, f_1 : 0.319; SMIC (SAMM): ar : 0.451, f_1 : 0.309	LOSO CV CD
Buhari et al. 2020	•	68	$S : L$	C	$F+E+G$	/	SVM	SMIC ar : 76.67%, f_1 : 0.75; CASME II ar : 75.04%, f_1 : 0.74; CAS(ME) ² ar : 81.85%, f_1 : 0.80; SAMM ar : 87.33%, f_1 : 0.87	LOSO CV
Zhou et al. 2020c	•	/	$AU : M$	$Optical-flow$ $+Inception$	L	GCN	$Softmax$	CASME II (SAMM) war : 0.708, uar : 0.595; SAMM (CASME II) war : 0.662, uar : 0.588; CASME II+SAMM f_1 : 0.685, wf_1 : 0.742)	LOSO CV CD
Liu et al. 2021	•	66	$S : R$	$Optical-flow$	KNN	$GraphSC$	SVM	SMIC ar : 70.51%, f_1 : 70.41%; CASME I (Yan et al. 2013) ar : 74.83%, f_1 : 74.95%; CASME II ar : 66.95%, f_1 : 69.11%	LOSO CV

¹ Prep.: processing; B.B.: bounding boxes; • = Yes, ○ = No; LM: landmarks.² Cat.: category; S/AU : {spatial; AU-level} representation; $L/B/M$: {landmark; label; map}-level graph; C : landmark coordinates; Φ : label distributions; L/F : {learning; fully} connections; E : Euclidean distance; G : Gradient using slope equation.³ Classif.: classifier; $GraphSC$: graph sparse coding; $G-TCN$: graph TCN.⁴ ar : average accuracy rate; f_1 : F1 score; war : weighted average recall; wf_1 : weighted F1 score; uar : unweighted average recall; (N) cl.: (N) affective classes; DB1 (DB2): train on DB2, test on DB1.⁵ CV: cross validation; LOSO: leave-one-subject-out; CD: cross database validation.

multaneously in many real cases. For example, furrowing on the forehead slightly and quickly when smiling indicates the true feeling of a person (Ekman and Friesen 1969). For another thing, since the evolutionary appearance information is crucial for the micro-expression analysis, building a spatio-temporal graph representation that can model the duration and the dynamic of micro-expressions is also a helpful but unexplored topic.

6.4 Special Tasks

The graph-based methods also play an important role in several special FAA tasks, such as pain detection (Kaltwang et al. 2015), non-basic emotion recognition (Zhang et al. 2019a), occluded FER (Dapogny et al. 2018; Zhou et al. 2020a), multi-modal emotion recognition (Chen et al. 2019; Chien et al. 2020) and emotion tagging (Xu et al. 2020b). Table 5 lists a summary of the latest graph-based FAA methods for special tasks. For graph constructions including two special representations (Chien et al. 2020; Xu et al. 2020b), the strategies of their node representations and edge initialization are similar to that in graph-based FER, MER and AUD methods. While for the reasoning step, GCN is the top-1 option. This observation implies that the framework

of the graph-based method discussed in this paper can be easily extended to many other FAA tasks and promote performance improvement.

7 Conclusion

In this survey, we expounded graph-based facial affect analysis methods by dissecting into fundamental components, and we discussed their potential and limitations. To conclude, we provide an overall discussion and highlight open directions.

7.1 Discussion

In this paper, we have focused on giving a general review into the appealing field of the graph-based FAA. We have started by introducing the fundamental preprocessing steps. An in-depth discussion about two major aspects have been followed, including the different kinds of graph-based affective representations and their corresponding relational reasoning models. Then, we have presented commonly used public databases. The representative recent studies have been summarized in terms of macro- and micro-expression recognition, action unit detection and other special FAA applications.

Table 5 Performance summary of graph-based methods for special FAA tasks discussed in this Paper

References	Prep. ¹		Representation ²			Reasoning		Database ³	Validation ⁴
	B.B.	LM	Cat.	Node	Edge	Model	Output		
Kaltwang et al. 2015	○	66	$S : \mathcal{L}$	C	L		LT	ShoulderPain (Lucey et al. 2011) <i>corr</i> : 0.23, <i>mse</i> : 0.60	8F CV
Dapogny et al. 2018	●	49	$S : \mathcal{L}$	C+HOG	Δ	AE	RF	CK+ (eyes occluded) <i>ar</i> : 87.9%; CK+ (mouth occluded) <i>ar</i> : 72.7%	10F-SI CV
Zhang et al. 2019a	●	/	$S : \mathcal{P}$	VGG	L	GCN	Softmax FC	EMOTIC (26 cl.) <i>prc</i> : 28.42%; EMOTIC (VAD) <i>er</i> : 0.9	HO
Chen et al. 2019	●	68	$ST : \mathcal{L}$	C	$\Delta+M$	GCN	FC	CES(Ringeval et al. 2019) <i>val_ccc</i> : 0.515, <i>aro_ccc</i> : 0.513	HO
Zhou et al. 2020a	●	44	$ST : \mathcal{L}$	C+HOG	$L+\mathbb{H}$	GCN	SoftMax	CK+ (random occlusion) <i>ar</i> : 95.51%; Oulu (random occlusion) <i>ar</i> : 81.21% AFEW (random occlusion) <i>ar</i> : 40.47%	10F-SI CV HO
Chien et al. 2020	○	/	\mathcal{O}	3DCNN	Trans. K	GCN	FC	Amigos (Correa et al. 2018) (Ascertain) <i>val_uar</i> : 0.798, <i>aro_uar</i> : 0.679; Ascertain (Subramanian et al. 2016) (Amigos) <i>val_uar</i> : 0.704, <i>aro_uar</i> : 0.569	CD
Xu et al. 2020b	○	/	\mathcal{O}	AE	Φ	GCN	GAN	NVIE (Wang et al. 2010) <i>ar</i> : 0.5632, f_1 : 0.6573, mif_1 : 0.6614, maf_1 : 0.6412; FilmStim (Schaefer et al. 2010) <i>ar</i> : 0.4669, f_1 : 0.5782, mif_1 : 0.6131, maf_1 : 0.5931	HO

¹ Prep.: processing; B.B.: bounding boxes; ● = Yes, ○ = No; LM: landmarks.² Cat.: category; $S/ST/\mathcal{O}$: {spatial; spatio-temporal; other} representation; \mathcal{L}/\mathcal{P} : {landmark; patch}-level graph; C: landmark coordinates; Φ : label distributions; Δ : triangulation; M/L : {manual/learning} connections; Trans. K : transfer knowledge.³ *corr*: Pearson correlation coefficient; *mes*: mean squared error; *prc*: area under the precision recall curves; *er*: average error rate; *val/aro*: valance/arousal; *ccc*: concordance correlation coefficient; *uar*: unweighted average recall; (N) cl.: (N) affective classes; VAD: valence, arousal, dominance; DB1 (DB2): train on DB2, test on DB1; *ar*: average accuracy rate; f_1 : F1 score; mif_1 : micro F1 score; maf_1 : macro F1 score.⁴ CV: cross validation; (K)F: k-folds; SI: subject independent; HO: holdout validation; CD: cross database validation.

7.1.1 Representation

When encoding facial affect into graph representations, strategies vary according to node elements and edge elements. Specifically, the spatial graph regards an affective face as multiple local crucial facial areas and model the relationship among them, while the spatio-temporal graph also considers the temporal evolution in continuous frames. Another distinctive representation is the AU-level graph. Since each AU and its co-occurrence dependency provide certain semantics of facial affects, most of the AU-level graphs are built by learning a distribution from existing available data. Other representations like multi-modal graphs employ the graph structure as a bridge to establish the information interaction from different modality.

There are various techniques for generating node attributes and initializing edge connections. The appearance and geometric information can be separately or jointly extracted by either pre-defined descriptors or deep models for each node, while the edge links can be obtained through manual linking, automatic learning or calculation rules. Regardless of these approaches, the node attribute generation and the edge connection initialization are followed by most methods. Therefore, spatial graphs and AU-level graphs are slightly different depending on the node element, but they can share

the similar node attributes (e.g., landmark coordinates (Liu et al. 2019; Li et al. 2019b)) or edge connections (e.g., KNN (Fan et al. 2020; Chen et al. 2020)). For the temporal domain, some methods also exploited the dynamic information in the representation stage (Xie et al. 2020a; Liu et al. 2021; Zhou et al. 2020c), even though they did not construct a whole space-time representation like spatio-temporal graphs.

7.1.2 Relational reasoning

Relational reasoning approaches infer latent relationships or inherent dependencies of graph nodes in terms of space, time, semantic, etc. The category of front graph representation will affect the technique choice of relational reasoning to a certain extent. Both traditional and advanced machine learning methods have been proposed to conduct the relational reasoning on affective graphs. DBNs explicitly update the relevant graph structure along with other pre-extracted local features and have been mostly used for AU-label representations. For deep learning methods, standard models can execute transformation of input format or adjustment of network architecture to meet the requirements of processing graph relational reasoning, while GNNs deal with structured graph data based on their specially designed architecture. The two types of deep

models can contribute to FAA either independently or cooperatively and are versatile for a variety of graph representations. Other basic machine learning methods, including graph structure learning and graph feature selection, have also been provided for relational reasoning, which have become less popular due to applicability and performance limitations.

7.2 Open Directions

Despite significant advances, the graph-based FAA is still an appealing field that has many open directions.

7.2.1 *In-the-wild scenarios*

Although many efforts have been done for graph-based FAA in naturalistic conditions (Yao et al. 2015; Dapogny et al. 2018; Chen et al. 2020; Liu et al. 2019; Xie et al. 2020a; Zhou et al. 2020a; Niu et al. 2019; Cui et al. 2020), even the state-of-the-art performance is far from actual applications. Factors like illumination, head pose and part occlusion are challenging in constructing an effective graph representation. For one thing, large illumination changes and head pose variations will impair the accuracy of face detection and registration, which is vital for establishing landmark-level graphs. The graph representation without landmarks (Yao et al. 2015; Xie et al. 2020b) should be a possible direction to avoid this problem. For another thing, missing face parts resulted by camera view or context occlusion make it difficult to encode enough facial information and obtain meaningful connections in an affective graph. Pioneer work (Dapogny et al. 2018; Zhou et al. 2020a) has tried to exploit a sub-graph without masked facial parts or generate adaptive edge links to alleviate the influence. Unfortunately, there still has been a big performance decrease compared to that in normal conditions. Therefore, more effective graph-based representations should be proposed to account for these problems.

7.2.2 *3D and 4D facial affects*

Using 3D and 4D face images might be another reasonable topic because the 3D face shape provides additional depth information and contains subtle facial deformations in a dynamic way, so that they are intuitively insensitive to pose and light changes. Some studies have transformed 3D faces to 2D images and generated graph representations (Dapogny et al. 2018; Corneanu et al. 2018; Li et al. 2019b; Fan et al. 2020), but they have not fully taken the advantage of the 3D data. Alternatively, attempts of both non-graph-based (Behzad et al. 2020) and graph-based methods (Pei and

Zha 2009) have been explored to directly conduct FAA on 3D or 4D faces. Since the structure of 3D face mesh is naturally close to the graph structure, employing the graph representation and reasoning to handle 3D face images will promote the improvement of in-the-wild FAA. Besides, there is also a potential topic of using 3D and 4D data with graph-based method in micro-expression recognition.

7.2.3 *Valence and arousal*

Estimating the continuous dimension is a rising topic in FAA. Not like discrete labels, the valence indicates the positive or negative characteristic of a facial affect, while the arousal denotes the intensity level of the activation about a facial affect. In recent years, some related competitions have been held at CVPR 2017 (Zafeiriou et al. 2017), BMVC 2019 (Kollias and Zafeiriou 2019) and FG 2020 (Kollias et al. 2020). And large-scale FAA databases (Aff-Wild I (Zafeiriou et al. 2017), II (Kollias et al. 2020)) containing V-A annotations have been released to support the continuous analysis of facial affects. Several graph-based methods have been proposed to perform the V-A measurement (Kaltwang et al. 2015; Walecki et al. 2017; Fan et al. 2020) on lab-controlled databases. Although methods like Zhang et al. (2019a) have reported V-A performance on in-the-wild databases, more comprehensive study should be done to reveal the effectiveness of graph-based methods in analysing continuous facial affects.

7.2.4 *Context and multi-modality*

Most current FAA methods only consider a single face in one image or one sequence. But in real cases, people usually have affective behaviors including facial expression, body gesture and emotional speaking (Huang et al. 2018). These facial affective displays are highly associated with context surroundings that include but not limited to the affective behavior of other people in social interactions or inanimate objects. Existing studies like Zhang et al. (2019a) and Xie et al. (2020b) have employed the graph reasoning to infer relationships between the target face and other objects in the same image. Future graph-based FAA methods should combine facial affects with other helpful context and perform the analysis on a fuller scope. Another reasonable topic is to introduce additional data channels that is multi-modality. The graph-based methods have also been successfully extended to process multi-modal affect analysis tasks with information such as audio (Chen et al. 2019) and physiological signal (Chien et al. 2020), which shows a good research prospect.

7.2.5 Cross-database and transfer learning

Insufficient annotations and imbalanced labels are two problems that limit the development of FAA research. One possible solution is to use the graph-based transfer learning. Efforts like [Niu et al. \(2019\)](#), [Cui et al. \(2020\)](#) and [Song et al. \(2021\)](#) have exploited the graph structure to solve this challenge in terms of semi-supervision, label correction and generation, or uncertainty measurement respectively. On the other hand, the performance of affective features extracted by using graph-based representation and reasoning has been proved through cross-database validation in all FER ([Chen et al. 2020](#); [Xie et al. 2020b](#)), MER ([Xie et al. 2020a](#); [Zhou et al. 2020c](#)) and AUD ([Tong et al. 2007](#); [Zhou et al. 2020c](#); [Cui et al. 2020](#)). This reveals that the graph-based method is valuable in improving the generalization capability of affective features.

References

- Aifanti N, Papachristou C, Delopoulos A (2010) The mug facial expression database. In: 11th International Workshop on Image Analysis for Multimedia Interactive Services WIAMIS 10, IEEE, pp 1–4
- Bai S, Kolter JZ, Koltun V (2018) An empirical evaluation of generic convolutional and recurrent networks for sequence modeling. arXiv preprint arXiv:180301271
- Behzad M, Vo N, Li X, Zhao G (2020) Landmarks-assisted collaborative deep framework for automatic 4d facial expression recognition. In: 15th IEEE International Conference on Automatic Face and Gesture Recognition (FG), IEEE, pp 1–5
- Ben X, Ren Y, Zhang J, Wang SJ, Kpalma K, Meng W, Liu YJ (2021) Video-based facial micro-expression analysis: A survey of datasets, features and algorithms. *IEEE Transactions on Pattern Analysis and Machine Intelligence* DOI 10.1109/TPAMI.2021.3067464
- Benitez-Quiroz CF, Srinivasan R, Feng Q, Wang Y, Martinez AM (2017) Emotionet challenge: Recognition of facial expressions of emotion in the wild. arXiv preprint arXiv:170301210
- Berkes P, Wood F, Pillow J (2008) Characterizing neural dependencies with copula models. In: International Conference on Neural Information Processing Systems (NeurIPS), vol 21, pp 129–136
- Bimler DL, Paramei GV (2006) Facial-expression affective attributes and their configural correlates: components and categories. *Spanish Journal of Psychology* 9(1):19
- Buhari AM, Ooi CP, Baskaran VM, Phan RC, Wong K, Tan WH (2020) Facs-based graph features for real-time micro-expression recognition. *Journal of Imaging* 6(12):130
- Bulat A, Tzimiropoulos G (2017) How far are we from solving the 2d and 3d face alignment problem?(and a dataset of 230,000 3d facial landmarks). In: IEEE International Conference on Computer Vision (ICCV), pp 1021–1030
- Calvo MG, Gutiérrez-García A, Del Líbano M (2018) What makes a smiling face look happy? visual saliency, distinctiveness, and affect. *Psychological Research* 82(2):296–309
- Carcagnì P, Del Coco M, Leo M, Distanto C (2015) Facial expression recognition and histograms of oriented gradients: a comprehensive study. SpringerPlus 4(1):1–25
- Chen H, Deng Y, Cheng S, Wang Y, Jiang D, Sahli H (2019) Efficient spatial temporal convolutional features for audiovisual continuous affect recognition. In: 9th International on Audio/Visual Emotion Challenge and Workshop, pp 19–26
- Chen S, Wang J, Chen Y, Shi Z, Geng X, Rui Y (2020) Label distribution learning on auxiliary label space graphs for facial expression recognition. In: IEEE Conference on Computer Vision and Pattern Recognition (CVPR), pp 13984–13993
- Chien WS, Yang HC, Lee CC (2020) Cross corpus physiological-based emotion recognition using a learnable visual semantic graph convolutional network. In: 28th ACM International Conference on Multimedia (ACM MM), pp 2999–3006
- Cootes TF, Edwards GJ, Taylor CJ (2001) Active appearance models. *IEEE Transactions on Pattern Analysis and Machine Intelligence* 23(6):681–685
- Corneanu C, Madadi M, Escalera S (2018) Deep structure inference network for facial action unit recognition. In: European Conference on Computer Vision (ECCV), pp 298–313
- Corneanu CA, Simón MO, Cohn JF, Guerrero SE (2016) Survey on rgb, 3d, thermal, and multimodal approaches for facial expression recognition: History, trends, and affect-related applications. *IEEE Transactions on Pattern Analysis and Machine Intelligence* 38(8):1548–1568
- Correa JAM, Abadi MK, Sebe N, Patras I (2018) Amigos: A dataset for affect, personality and mood research on individuals and groups. *IEEE Transactions on Affective Computing* DOI 10.1109/TAFFC.2018.2884461
- Cui Z, Zhang Y, Ji Q (2020) Label error correction and generation through label relationships. In: AAAI Conference on Artificial Intelligence (AAAI), vol 34,

- pp 3693–3700
- Dalal N, Triggs B (2005) Histograms of oriented gradients for human detection. In: 2005 IEEE Conference on Computer Vision and Pattern Recognition (CVPR), Ieee, vol 1, pp 886–893
- Dapogny A, Bailly K, Dubuisson S (2018) Confidence-weighted local expression predictions for occlusion handling in expression recognition and action unit detection. *International Journal of Computer Vision* 126(2):255–271
- Darwin C, Prodger P (1998) *The expression of the emotions in man and animals*. Oxford University Press, USA
- Davison AK, Lansley C, Costen N, Tan K, Yap MH (2018) Sann: A spontaneous micro-facial movement dataset. *IEEE Transactions on Affective Computing* 9(1):116–129
- Defferrard M, Bresson X, Vandergheynst P (2016) Convolutional neural networks on graphs with fast localized spectral filtering. In: *International Conference on Neural Information Processing Systems (NeurIPS)*, pp 3837–3845
- Derkach D, Sukno FM (2017) Local shape spectrum analysis for 3d facial expression recognition. In: *12th IEEE International Conference on Automatic Face and Gesture Recognition (FG)*, IEEE, pp 41–47
- Dhall A, Ramana Murthy O, Goecke R, Joshi J, Gedeon T (2015) Video and image based emotion recognition challenges in the wild: EmotiW 2015. In: *2015 ACM on International Conference on Multimodal Interaction (ICMI)*, pp 423–426
- Dhall A, Goecke R, Ghosh S, Joshi J, Hoey J, Gedeon T (2017) From individual to group-level emotion recognition: EmotiW 5.0. In: *19th ACM International Conference on Multimodal Interaction (ICMI)*, pp 524–528
- Dhall A, Sharma G, Goecke R, Gedeon T (2020) EmotiW 2020: Driver gaze, group emotion, student engagement and physiological signal based challenges. In: *2020 International Conference on Multimodal Interaction*, pp 784–789
- Dong X, Yang Y, Wei SE, Weng X, Sheikh Y, Yu SI (2020) Supervision by registration and triangulation for landmark detection. *IEEE Transactions on Pattern Analysis and Machine Intelligence* DOI 10.1109/TPAMI.2020.2983935
- Durmuşoğlu A, Kahraman Y (2016) Facial expression recognition using geometric features. In: *2016 International Conference on Systems, Signals and Image Processing (IWSSIP)*, IEEE, pp 1–5
- Ekman P (1994) Strong evidence for universals in facial expressions: a reply to russell’s mistaken critique. *Psychological Bulletin* 115(2):268–287
- Ekman P (2002) *Facial action coding system (facs)*. A Human Face
- Ekman P, Friesen WV (1969) Nonverbal leakage and clues to deception. *Psychiatry* 32(1):88–106
- Ekman P, Friesen WV (1971) Constants across cultures in the face and emotion. *Journal of Personality and Social Psychology* 17(2):124–129
- Fabian Benitez-Quiroz C, Srinivasan R, Martinez AM (2016) Emotionet: An accurate, real-time algorithm for the automatic annotation of a million facial expressions in the wild. In: *IEEE Conference on Computer Vision and Pattern Recognition (CVPR)*, pp 5562–5570
- Fan Y, Lam J, Li V (2020) Facial action unit intensity estimation via semantic correspondence learning with dynamic graph convolution. In: *AAAI Conference on Artificial Intelligence (AAAI)*, vol 34, pp 12701–12708
- Feng ZH, Kittler J, Awais M, Huber P, Wu XJ (2017) Face detection, bounding box aggregation and pose estimation for robust facial landmark localisation in the wild. In: *IEEE Conference on Computer Vision and Pattern Recognition workshops (CVPRW)*, pp 160–169
- Friesen E, Ekman P (1978) *Facial action coding system: a technique for the measurement of facial movement*. Palo Alto 3(2):5
- Gazzaniga MS, Ivry RB, Mangun G (2006) *Cognitive Neuroscience. The Biology of the Mind*, (2014). Norton: New York
- Goh KM, Ng CH, Lim LL, Sheikh UU (2020) Micro-expression recognition: an updated review of current trends, challenges and solutions. *The Visual Computer* 36(3):445–468
- Goodfellow IJ, Erhan D, Carrier PL, Courville A, Mirza M, Hamner B, Cukierski W, Tang Y, Thaler D, Lee DH, et al. (2015) Challenges in representation learning: A report on three machine learning contests. *Neural Networks* 64:59–63
- Greenwald MK, Cook EW, Lang PJ (1989) Affective judgment and psychophysiological response: dimensional covariation in the evaluation of pictorial stimuli. *Journal of Psychophysiology* 3(1):51–64
- Haggard EA, Isaacs KS (1966) Micromomentary facial expressions as indicators of ego mechanisms in psychotherapy. In: *Methods of Research in Psychotherapy*, Springer, pp 154–165
- Hara K, Kataoka H, Satoh Y (2018) Can spatiotemporal 3d cnns retrace the history of 2d cnns and imagenet? In: *IEEE Conference on Computer Vision and Pattern Recognition (CVPR)*, pp 6546–6555
- Hassan AK, Mohammed SN (2020) A novel facial emotion recognition scheme based on graph mining. De-

- fence Technology 16(5):1062–1072
- He K, Zhang X, Ren S, Sun J (2016) Deep residual learning for image recognition. In: IEEE Conference on Computer Vision and Pattern Recognition (CVPR), pp 770–778
- He T, Jin X (2019) Image emotion distribution learning with graph convolutional networks. In: 2019 International Conference on Multimedia Retrieval (ICMR), pp 382–390
- Huang X, Dhall A, Goecke R, Pietikäinen M, Zhao G (2018) Multimodal framework for analyzing the affect of a group of people. IEEE Transactions on Multimedia 20(10):2706–2721
- Jack RE, Garrod OG, Yu H, Caldara R, Schyns PG (2012) Facial expressions of emotion are not culturally universal. National Academy of Sciences 109(19):7241–7244
- Kakumanu P, Bourbakis N (2006) A local-global graph approach for facial expression recognition. In: 18th IEEE International Conference on Tools with Artificial Intelligence (ICTAI), IEEE, pp 685–692
- Kaltwang S, Todorovic S, Pantic M (2015) Latent trees for estimating intensity of facial action units. In: IEEE Conference on Computer Vision and Pattern Recognition (CVPR), pp 296–304
- Kanade T, Cohn JF, Tian Y (2000) Comprehensive database for facial expression analysis. In: 4th IEEE International Conference on Automatic Face and Gesture Recognition (FG), IEEE, pp 46–53
- Kazemi V, Sullivan J (2014) One millisecond face alignment with an ensemble of regression trees. In: IEEE Conference on Computer Vision and Pattern Recognition (CVPR), pp 1867–1874
- Kemp C, Tenenbaum JB (2008) The discovery of structural form. National Academy of Sciences 105(31):10687–10692
- Khorrami P, Le Paine T, Brady K, Dagli C, Huang TS (2016) How deep neural networks can improve emotion recognition on video data. In: 2016 IEEE International Conference on Image Processing (ICIP), IEEE, pp 619–623
- Kipf TN, Welling M (2017) Semi-supervised classification with graph convolutional networks. In: 5th International Conference on Learning Representations (ICLR)
- Kirsch RA (1971) Computer determination of the constituent structure of biological images. Computers and Biomedical Research 4(3):315–328
- Kollias D, Zafeiriou S (2019) Expression, affect, action unit recognition: Aff-wild2, multi-task learning and arcfac. arXiv preprint arXiv:191004855
- Kollias D, Tzirakis P, Nicolaou MA, Papaioannou A, Zhao G, Schuller B, Kotsia I, Zafeiriou S (2019) Deep affect prediction in-the-wild: Aff-wild database and challenge, deep architectures, and beyond. International Journal of Computer Vision 127(6):907–929
- Kollias D, Schulc A, Hajiyev E, Zafeiriou S (2020) Analysing affective behavior in the first abaw 2020 competition. In: 15th IEEE International Conference on Automatic Face and Gesture Recognition (FG), IEEE Computer Society, pp 794–800
- Kosti R, Alvarez JM, Recasens A, Lapedriza A (2019) Context based emotion recognition using emotic dataset. IEEE Transactions on Pattern Analysis and Machine Intelligence 42(11):2755–2766
- Kotsia I, Pitas I (2006) Facial expression recognition in image sequences using geometric deformation features and support vector machines. IEEE Transactions on Image Processing 16(1):172–187
- Kung HW, Tu YH, Hsu CT (2015) Dual subspace non-negative graph embedding for identity-independent expression recognition. IEEE Transactions on Information Forensics and Security 10(3):626–639
- Lei L, Li J, Chen T, Li S (2020) A novel graph-tcn with a graph structured representation for micro-expression recognition. In: 28th ACM International Conference on Multimedia (ACM MM), pp 2237–2245
- Li B, Li X, Zhang Z, Wu F (2019a) Spatio-temporal graph routing for skeleton-based action recognition. In: AAAI Conference on Artificial Intelligence (AAAI), vol 33, pp 8561–8568
- Li G, Zhu X, Zeng Y, Wang Q, Lin L (2019b) Semantic relationships guided representation learning for facial action unit recognition. In: AAAI Conference on Artificial Intelligence (AAAI), vol 33, pp 8594–8601
- Li S, Deng W (2019) Reliable crowdsourcing and deep locality-preserving learning for unconstrained facial expression recognition. IEEE Transactions on Image Processing 28(1):356–370
- Li S, Deng W (2020) Deep facial expression recognition: A survey. IEEE Transactions on Affective Computing DOI 10.1109/TAFFC.2020.2981446
- Li W, Abtahi F, Zhu Z, Yin L (2017) Eac-net: A region-based deep enhancing and cropping approach for facial action unit detection. In: 12th IEEE International Conference on Automatic Face and Gesture Recognition (FG), IEEE, pp 103–110
- Li X, Pfister T, Huang X, Zhao G, Pietikäinen M (2013) A spontaneous micro-expression database: Inducement, collection and baseline. In: 10th IEEE International Conference and Workshops on Automatic Face and Gesture Recognition (FG), IEEE, pp 1–6
- Li Y, Gupta A (2018) Beyond grids: Learning graph representations for visual recognition. In: International Conference on Neural Information Processing

- Systems (NeurIPS), pp 9245–9255
- Li Y, Tarlow D, Brockschmidt M, Zemel R (2016) Gated graph sequence neural networks. In: 4th International Conference on Learning Representations (ICLR), pp 1–20
- Liu C, Wechsler H (2003) Independent component analysis of gabor features for face recognition. *IEEE Transactions on Neural Networks* 14(4):919–928
- Liu D, Zhang H, Zhou P (2020a) Video-based facial expression recognition using graph convolutional networks. arXiv preprint arXiv:201013386
- Liu Y, Zhang X, Lin Y, Wang H (2019) Facial expression recognition via deep action units graph network based on psychological mechanism. *IEEE Transactions on Cognitive and Developmental Systems* 12(2):311–322
- Liu YJ, Zhang JK, Yan WJ, Wang SJ, Zhao G, Fu X (2015) A main directional mean optical flow feature for spontaneous micro-expression recognition. *IEEE Transactions on Affective Computing* 7(4):299–310
- Liu YJ, Li BJ, Lai YK (2021) Sparse mdmo: Learning a discriminative feature for spontaneous micro-expression recognition. *IEEE Transactions on Affective Computing* 12(1):254–261
- Liu Z, Dong J, Zhang C, Wang L, Dang J (2020b) Relation modeling with graph convolutional networks for facial action unit detection. In: International Conference on Multimedia Modeling, Springer, pp 489–501
- Lo L, Xie HX, Shuai HH, Cheng WH (2020) Mer-gen: Micro-expression recognition based on relation modeling with graph convolutional networks. In: 2020 IEEE Conference on Multimedia Information Processing and Retrieval (MIPR), IEEE, pp 79–84
- Lowe DG (2004) Distinctive image features from scale-invariant keypoints. *International Journal of Computer Vision* 60(2):91–110
- Lucey P, Cohn JF, Kanade T, Saragih J, Ambadar Z, Matthews I (2010) The extended cohn-kanade dataset (ck+): A complete dataset for action unit and emotion-specified expression. In: 2010 IEEE Conference on Computer Vision and Pattern Recognition-Workshops, IEEE, pp 94–101
- Lucey P, Cohn JF, Prkachin KM, Solomon PE, Matthews I (2011) Painful data: The unbc-mcmaster shoulder pain expression archive database. In: 2011 IEEE International Conference on Automatic Face and Gesture Recognition (FG), IEEE, pp 57–64
- Luo Z, Liu L, Yin J, Li Y, Wu Z (2017) Deep learning of graphs with ngram convolutional neural networks. *IEEE Transactions on Knowledge and Data Engineering* 29(10):2125–2139
- Lyons MJ, Budynek J, Akamatsu S (1999) Automatic classification of single facial images. *IEEE Transactions on Pattern Analysis and Machine Intelligence* 21(12):1357–1362
- Lyons MJ, Budynek J, Plante A, Akamatsu S (2000) Classifying facial attributes using a 2-d gabor wavelet representation and discriminant analysis. In: 4th IEEE International Conference on Automatic Face and Gesture Recognition (FG), IEEE, pp 202–207
- Martinez B, Valstar MF, Jiang B, Pantic M (2017) Automatic analysis of facial actions: A survey. *IEEE Transactions on Affective Computing* 10(3):325–347
- Masi I, Wu Y, Hassner T, Natarajan P (2018) Deep face recognition: A survey. In: 2018 31st SIBGRAPI Conference on Graphics, Patterns and Images (SIBGRAPI), IEEE, pp 471–478
- Mavadati SM, Mahoor MH, Bartlett K, Trinh P, Cohn JF (2013) Disfa: A spontaneous facial action intensity database. *IEEE Transactions on Affective Computing* 4(2):151–160
- Meena HK, Sharma KK, Joshi SD (2018) Facial expression recognition using the spectral graph wavelet. *IET Signal Processing* 13(2):224–229
- Mohseni S, Zarei N, Ramazani S (2014) Facial expression recognition using anatomy based facial graph. In: 2014 IEEE International Conference on Systems, Man, and Cybernetics (SMC), IEEE, pp 3715–3719
- Mollahosseini A, Chan D, Mahoor MH (2016) Going deeper in facial expression recognition using deep neural networks. In: 2016 IEEE Winter Conference on Applications of Computer Vision (WACV), IEEE, pp 1–10
- Mollahosseini A, Hasani B, Mahoor MH (2019) Affectnet: A database for facial expression, valence, and arousal computing in the wild. *IEEE Transactions on Affective Computing* 10(1):18–31
- Niu X, Han H, Shan S, Chen X (2019) Multi-label co-regularization for semi-supervised facial action unit recognition. In: International Conference on Neural Information Processing Systems (NeurIPS), vol 32, pp 1–11
- Oh YH, See J, Le Ngo AC, Phan RCW, Baskaran VM (2018) A survey of automatic facial micro-expression analysis: databases, methods, and challenges. *Frontiers in Psychology* 9:1128
- Pei Y, Zha H (2009) 3d facial expression editing based on the dynamic graph model. In: 2009 IEEE International Conference on Multimedia and Expo (ICME), IEEE, pp 1354–1357
- Picard RW, Vyzas E, Healey J (2001) Toward machine emotional intelligence: Analysis of affective physiological state. *IEEE Transactions on Pattern Analysis and Machine Intelligence* 23(10):1175–1191
- Plutchik R (1980) A general psychoevolutionary theory of emotion. In: *Theories of Emotion*, Elsevier, pp 3–

33

- Qiu Z, Yao T, Mei T (2017) Learning spatio-temporal representation with pseudo-3d residual networks. In: IEEE International Conference on Computer Vision (ICCV), pp 5533–5541
- Qu F, Wang SJ, Yan WJ, Li H, Wu S, Fu X (2018) Cas(me)² : A database for spontaneous macro-expression and micro-expression spotting and recognition. *IEEE Transactions on Affective Computing* 9(4):424–436
- Ranjan R, Patel VM, Chellappa R (2017) Hyperface: A deep multi-task learning framework for face detection, landmark localization, pose estimation, and gender recognition. *IEEE Transactions on Pattern Analysis and Machine Intelligence* 41(1):121–135
- Ren S, He K, Girshick R, Sun J (2016) Faster r-cnn: towards real-time object detection with region proposal networks. *IEEE Transactions on Pattern Analysis and Machine Intelligence* 39(6):1137–1149
- Ringeval F, Schuller B, Valstar M, Cummins N, Cowie R, Tavabi L, Schmitt M, Alisamir S, Amiriparian S, Messner EM, et al. (2019) Avec 2019 workshop and challenge: state-of-mind, detecting depression with ai, and cross-cultural affect recognition. In: 9th International on Audio/Visual Emotion Challenge and Workshop, pp 3–12
- Rivera AR, Chae O (2015) Spatiotemporal directional number transitional graph for dynamic texture recognition. *IEEE Transactions on Pattern Analysis and Machine Intelligence* 37(10):2146–2152
- Rouast PV, Adam M, Chiong R (2019) Deep learning for human affect recognition: Insights and new developments. *IEEE Transactions on Affective Computing*
- Russell JA (1978) Evidence of convergent validity on the dimensions of affect. *Journal of Personality and Social Psychology* 36(10):1152
- Sabzevari M, Toosizadeh S, Quchani SR, Abrishami V (2010) A fast and accurate facial expression synthesis system for color face images using face graph and deep belief network. In: 2010 International Conference on Electronics and Information Engineering, IEEE, vol 2, pp V2–354
- Sariyanidi E, Gunes H, Cavallaro A (2014) Automatic analysis of facial affect: A survey of registration, representation, and recognition. *IEEE Transactions on Pattern Analysis and Machine Intelligence* 37(6):1113–1133
- Schaefer A, Nils F, Sanchez X, Philippot P (2010) Assessing the effectiveness of a large database of emotion-eliciting films: A new tool for emotion researchers. *Cognition and Emotion* 24(7):1153–1172
- Sechkova T, Tonchev K, Manolova A (2016) Action unit recognition in still images using graph-based feature selection. In: 2016 IEEE 8th International Conference on Intelligent Systems (IS), IEEE, pp 646–650
- Simonyan K, Zisserman A (2014) Very deep convolutional networks for large-scale image recognition. arXiv preprint arXiv:1409.1556
- Song T, Chen L, Zheng W, Ji Q (2021) Uncertain graph neural networks for facial action unit detection. In: AAAI Conference on Artificial Intelligence (AAAI), pp 1–10
- Stappen L, Baird A, Rizos G, Tzirakis P, Du X, Hafner F, Schumann L, Mallol-Ragolta A, Schuller BW, Lefter I, et al. (2020) Muse 2020 challenge and workshop: Multimodal sentiment analysis, emotion-target engagement and trustworthiness detection in real-life media: Emotional car reviews in-the-wild. In: 1st International on Multimodal Sentiment Analysis in Real-life Media Challenge and Workshop, pp 35–44
- Subramanian R, Wache J, Abadi MK, Vieriu RL, Winkler S, Sebe N (2016) Ascertain: Emotion and personality recognition using commercial sensors. *IEEE Transactions on Affective Computing* 9(2):147–160
- Tanchotsrinon C, Phimoltares S, Maneeroj S (2011) Facial expression recognition using graph-based features and artificial neural networks. In: 2011 IEEE International Conference on Imaging Systems and Techniques, IEEE, pp 331–334
- Tavakolian M, Hadid A (2019) A spatiotemporal convolutional neural network for automatic pain intensity estimation from facial dynamics. *International Journal of Computer Vision* 127(10):1413–1425
- Tian YI, Kanade T, Cohn JF (2001) Recognizing action units for facial expression analysis. *IEEE Transactions on Pattern Analysis and Machine Intelligence* 23(2):97–115
- Tong Y, Liao W, Ji Q (2007) Facial action unit recognition by exploiting their dynamic and semantic relationships. *IEEE Transactions on Pattern Analysis and Machine Intelligence* 29(10):1683–1699
- Tran D, Wang H, Torresani L, Ray J, LeCun Y, Paluri M (2018) A closer look at spatiotemporal convolutions for action recognition. In: IEEE Conference on Computer Vision and Pattern Recognition (CVPR), pp 6450–6459
- Valstar M, Pantic M (2010) Induced disgust, happiness and surprise: an addition to the mmi facial expression database. In: 3rd International Workshop on EMOTION: Corpora for Research on Emotion and Affect, Paris, France, p 65
- Valstar MF, Jiang B, Mehu M, Pantic M, Scherer K (2011) The first facial expression recognition and analysis challenge. In: 2011 IEEE International Conference on Automatic Face and Gesture Recognition (FG), IEEE, pp 921–926

- Valstar MF, Almaev T, Girard JM, McKeown G, Mehu M, Yin L, Pantic M, Cohn JF (2015) Fera 2015-second facial expression recognition and analysis challenge. In: 2015 11th IEEE International Conference and Workshops on Automatic Face and Gesture Recognition (FG), IEEE, vol 6, pp 1–8
- Veličković P, Cucurull G, Casanova A, Romero A, Lio P, Bengio Y (2017) Graph attention networks. arXiv preprint arXiv:171010903
- Viola P, Jones M (2001) Rapid object detection using a boosted cascade of simple features. In: 2001 IEEE Conference on Computer Vision and Pattern Recognition (CVPR), IEEE, vol 1, pp I–I
- Walecki R, Rudovic O, Pavlovic V, Schuller B, Pantic M (2017) Deep structured learning for facial expression intensity estimation. *Image and Vision Computing* 259:143–154
- Wang J, Sun K, Cheng T, Jiang B, Deng C, Zhao Y, Liu D, Mu Y, Tan M, Wang X, et al. (2020) Deep high-resolution representation learning for visual recognition. *IEEE Transactions on Pattern Analysis and Machine Intelligence* DOI 10.1109/TPAMI.2020.2983686
- Wang N, Gao X, Tao D, Yang H, Li X (2018) Facial feature point detection: A comprehensive survey. *Neurocomputing* 275:50–65
- Wang S, Liu Z, Lv S, Lv Y, Wu G, Peng P, Chen F, Wang X (2010) A natural visible and infrared facial expression database for expression recognition and emotion inference. *IEEE Transactions on Multimedia* 12(7):682–691
- Wang Y, Sun Y, Liu Z, Sarma SE, Bronstein MM, Solomon JM (2019) Dynamic graph cnn for learning on point clouds. *ACM Transactions On Graphics* 38(5):1–12
- Wu C, Chai L, Yang J, Sheng Y (2019) Facial expression recognition using convolutional neural network on graphs. In: 2019 Chinese Control Conference (CCC), IEEE, pp 7572–7576
- Xiao B, Wu H, Wei Y (2018) Simple baselines for human pose estimation and tracking. In: European Conference on Computer Vision (ECCV), pp 466–481
- Xie HX, Lo L, Shuai HH, Cheng WH (2020a) Assisted graph attention convolutional network for micro-expression recognition. In: 28th ACM International Conference on Multimedia (ACM MM), pp 2871–2880
- Xie Y, Chen T, Pu T, Wu H, Lin L (2020b) Adversarial graph representation adaptation for cross-domain facial expression recognition. In: 28th ACM International Conference on Multimedia (ACM MM), pp 1255–1264
- Xu Y, Yan W, Yang G, Luo J, Li T, He J (2020a) Centerface: joint face detection and alignment using face as point. *Scientific Programming* DOI 10.1155/2020/7845384
- Xu Z, Wang S, Wang C (2020b) Exploiting multi-emotion relations at feature and label levels for emotion tagging. In: 28th ACM International Conference on Multimedia (ACM MM), pp 2955–2963
- Yan WJ, Wu Q, Liu YJ, Wang SJ, Fu X (2013) Casme database: a dataset of spontaneous micro-expressions collected from neutralized faces. In: 10th IEEE International Conference and workshops on Automatic Face and Gesture Recognition (FG), IEEE, pp 1–7
- Yan WJ, Li X, Wang SJ, Zhao G, Liu YJ, Chen YH, Fu X (2014) Casme ii: An improved spontaneous micro-expression database and the baseline evaluation. *PLoS One* 9(1):e86041
- Yao A, Shao J, Ma N, Chen Y (2015) Capturing unaware facial features and their latent relations for emotion recognition in the wild. In: 2015 ACM on International Conference on Multimodal Interaction (ICMI), pp 451–458
- Yin L, Wei X, Sun Y, Wang J, Rosato MJ (2006) A 3d facial expression database for facial behavior research. In: 7th International Conference on Automatic Face and Gesture Recognition (FG), IEEE, pp 211–216
- Yin L, Chen X, Sun Y, Worm T, Reale M (2008) A high-resolution 3d dynamic facial expression database. In: 8th IEEE International Conference on Automatic Face and Gesture Recognition (FG), pp 1–6
- Yu Z, Zhang C (2015) Image based static facial expression recognition with multiple deep network learning. In: 2015 ACM on International Conference on Multimodal Interaction (ICMI), pp 435–442
- Zafeiriou S, Pitas I (2008) Discriminant graph structures for facial expression recognition. *IEEE Transactions on Multimedia* 10(8):1528–1540
- Zafeiriou S, Kollias D, Nicolaou MA, Papaioannou A, Zhao G, Kotsia I (2017) Aff-wild: valence and arousal ‘in-the-wild’ challenge. In: IEEE Conference on Computer Vision and Pattern Recognition Workshops (CVPRW), pp 34–41
- Zhang K, Zhang Z, Li Z, Qiao Y (2016) Joint face detection and alignment using multitask cascaded convolutional networks. *IEEE Signal Processing Letters* 23(10):1499–1503
- Zhang K, Huang Y, Du Y, Wang L (2017) Facial expression recognition based on deep evolutionary spatial-temporal networks. *IEEE Transactions on Image Processing* 26(9):4193–4203
- Zhang L, Verma B, Tjondronegoro D, Chandran V (2018a) Facial expression analysis under partial oc-

- clusion: A survey. *ACM Computing Surveys (CSUR)* 51(2):1–49
- Zhang M, Liang Y, Ma H (2019a) Context-aware affective graph reasoning for emotion recognition. In: 2019 IEEE International Conference on Multimedia and Expo (ICME), IEEE, pp 151–156
- Zhang X, Yin L, Cohn JF, Canavan S, Reale M, Horowitz A, Liu P, Girard JM (2014) Bp4d-spontaneous: a high-resolution spontaneous 3d dynamic facial expression database. *Image and Vision Computing* 32(10):692–706
- Zhang Y, Pal S, Coates M, Ustebay D (2019b) Bayesian graph convolutional neural networks for semi-supervised classification. In: *AAAI Conference on Artificial Intelligence (AAAI)*, vol 33, pp 5829–5836
- Zhang Z, Luo P, Loy CC, Tang X (2018b) From facial expression recognition to interpersonal relation prediction. *International Journal of Computer Vision* 126(5):550–569
- Zhang Z, Wang T, Yin L (2020) Region of interest based graph convolution: A heatmap regression approach for action unit detection. In: 28th ACM International Conference on Multimedia (ACM MM), pp 2890–2898
- Zhao G, Li X (2019) Automatic micro-expression analysis: open challenges. *Frontiers in Psychology* 10:1833
- Zhao G, Pietikainen M (2007) Dynamic texture recognition using local binary patterns with an application to facial expressions. *IEEE Transactions on Pattern Analysis and Machine Intelligence* 29(6):915–928
- Zhao G, Huang X, Taini M, Li SZ, Pietikäinen M (2011) Facial expression recognition from near-infrared videos. *Image and Vision Computing* 29(9):607–619
- Zhao K, Chu WS, Zhang H (2016) Deep region and multi-label learning for facial action unit detection. In: *IEEE Conference on Computer Vision and Pattern Recognition (CVPR)*, pp 3391–3399
- Zhao L, Peng X, Tian Y, Kapadia M, Metaxas DN (2020) Towards image-to-video translation: A structure-aware approach via multi-stage generative adversarial networks. *International Journal of Computer Vision* 128(10):2514–2533
- Zheng W, Zhou X, Zou C, Zhao L (2006) Facial expression recognition using kernel canonical correlation analysis (kcca). *IEEE Transactions on Neural Networks* 17(1):233–238
- Zhi R, Flierl M, Ruan Q, Kleijn WB (2010) Graph-preserving sparse nonnegative matrix factorization with application to facial expression recognition. *IEEE Transactions on Systems, Man, and Cybernetics, Part B (Cybernetics)* 41(1):38–52
- Zhi R, Liu M, Zhang D (2020) A comprehensive survey on automatic facial action unit analysis. *The Visual Computer* 36(5):1067–1093
- Zhong L, Bai C, Li J, Chen T, Li S, Liu Y (2019) A graph-structured representation with brnn for static-based facial expression recognition. In: 14th IEEE International Conference on Automatic Face and Gesture Recognition (FG), IEEE, pp 1–5
- Zhou J, Zhang X, Liu Y (2020a) Learning the connectivity: Situational graph convolution network for facial expression recognition. In: 2020 IEEE International Conference on Visual Communications and Image Processing (VCIP), IEEE, pp 230–234
- Zhou J, Zhang X, Liu Y, Lan X (2020b) Facial expression recognition using spatial-temporal semantic graph network. In: 2020 IEEE International Conference on Image Processing (ICIP), IEEE, pp 1961–1965
- Zhou L, Mao Q, Xue L (2019) Dual-inception network for cross-database micro-expression recognition. In: 14th IEEE International Conference on Automatic Face and Gesture Recognition (FG), IEEE, pp 1–5
- Zhou L, Mao Q, Dong M (2020c) Objective class-based micro-expression recognition through simultaneous action unit detection and feature aggregation. *arXiv preprint arXiv:201213148*
- Zhu X, Ramanan D (2012) Face detection, pose estimation, and landmark localization in the wild. In: 2012 IEEE Conference on Computer Vision and Pattern Recognition (CVPR), IEEE, pp 2879–2886
- Zhu Y, Wang S, Yue L, Ji Q (2014) Multiple-facial action unit recognition by shared feature learning and semantic relation modeling. In: 22nd International Conference on Pattern Recognition (ICPR), IEEE, pp 1663–1668